hydrology

MDPI

Article

Index-Based Vulnerability Assessment—A Multi-Dimensional Index as a Tool for Capturing the Effects of Nature-Based Solutions for Flood Mitigation

Jelena Kovačević-Majkić [1], Nikola Rosić [2], Dragoljub Štrbac [1], Vujica Šarenac [3] and Andrijana Todorović [2,*]

[1] Geographical Institute "Jovan Cvijić" of the Serbian Academy of Sciences and Arts, 11000 Belgrade, Serbia; j.kovacevic@gi.sanu.ac.rs (J.K.-M.); d.strbac@gi.sanu.ac.rs (D.Š.)
[2] Faculty of Civil Engineering, University of Belgrade, 11000 Belgrade, Serbia; nrosic@grf.bg.ac.rs
[3] IWA Consulting, 11000 Belgrade, Serbia; vujica.sarenac@iwa-cons.com
* Correspondence: atodorovic@grf.bg.ac.rs

Abstract

This study presents the Multi-dimensional Flood Vulnerability Index (M-FLOVI), calculated by using an index-based method specifically tailored to capture the impact of nature-based solutions (NbSs) on vulnerability. It aggregates five vulnerability dimensions (physical, economic, environmental, social and institutional) into a single index within a multi-level framework. Each dimension is calculated from a set of indicators that can be computed with moderate data demands. These calculations generally require information about buildings, infrastructure, land cover, population, protected areas and cultural heritage, which can partly be obtained from open-access data. M-FLOVI ranges between 0 and 1, and it can be readily mapped and combined with flood hazard to produce flood risk maps. This paper elaborates a step-by-step M-FLOVI calculation in the Tamnava River Basin, Serbia, where various NbSs were proposed. Under the baseline conditions, most of the study area exhibits either moderate (83.5%) or low vulnerability (15.8%). These NbSs decrease future vulnerability in 6.6 km^2 (1.34%) of the study area. Afforestation (0.59%) and retention ponds (0.42%) decrease environmental vulnerability, while flood plain restoration (0.33%), which is expected to create a protected bird habitat, increases environmental vulnerability. These results suggest that M-FLOVI can effectively capture NbSs' impacts on future vulnerability to floods.

Keywords: index-based method; flood risk assessment; large-scale NbS; natural flood management; vulnerability

Check for updates

Academic Editor: Evangelos Rozos

Received: 9 May 2026
Revised: 1 July 2026
Accepted: 2 July 2026
Published: 7 July 2026

Copyright: © 2026 by the authors. Licensee MDPI, Basel, Switzerland. This article is an open access article distributed under the terms and conditions of the Creative Commons Attribution (CC BY) license.

1. Introduction

In the atmosphere of frequent and devastating floods that repeatedly cause casualties and substantial economic losses worldwide [1–4], societies have become aware of the necessity to reduce vulnerability to floods [3]. In this sense, various flood risk management (FRM) measures are implemented, where flood risk and vulnerability assessments play a pivotal role in assisting authorities to prioritize measures' implementation [5–7]. Vulnerability assessments can increase the effectiveness of FRM by focusing on the areas with many exposed and vulnerable elements (people, assets and natural resources), since these determine whether a flood becomes a natural disaster. Precise vulnerability assessments are, therefore, essential for effective and sustainable FRM.

Generally, FRM relies on measures that enhance flood resilience and/or reduce vulnerability, together with hazard reduction. Alongside conventional grey measures widely implemented for FRM [8–10], nature-based solutions (NbSs) have increasingly been recognized as a desirable and convenient option for flood risk reduction both in small urban settings and at larger scales [11–13]. Implementation of NbSs has been advocated as they can provide co-benefits, such as carbon sequestration, CO_2 emission reduction, improvement of air quality, biological control, creation of new habitats or recreational opportunities, in addition to flood risk reduction [11]. However, the implementation of measures such as afforestation, retention ponds or floodplain restoration changes land cover and can thus reduce vulnerability to floods in the area of interest. In other words, NbSs can reduce flood risk by decreasing both hazard and vulnerability. Therefore, when evaluating NbSs' effectiveness in reducing flood risk by comparing post-intervention flood risk to that under pre-intervention (baseline) conditions, both of them have to be assessed with their respective vulnerabilities. However, dynamic changes in vulnerability to floods, especially those caused by the NbSs' implementation, are largely neglected [14], and future flood risk (i.e., in the post-intervention state) is generally assessed based on vulnerability obtained under baseline conditions [15].

Assessing vulnerability to floods remains a challenging task for decision making, as it requires a balance between theoretical comprehensiveness and practical applicability [16]. Consequently, there is no standardized, generally accepted approach to vulnerability assessment [17]. Currently used approaches for quantitative vulnerability assessments can generally be grouped into four categories: the vulnerability curve method, the disaster loss method, modeling methods and index-based methods [17,18]. Among these, index-based methods are particularly appealing due to the considerable flexibility they offer. Specifically, they allow various vulnerability dimensions to be taken into account or omitted to reflect region-specific conditions, as opposed to other methods with rigidly predefined structures (i.e., vulnerability dimensions and relationships among them).

The index-based vulnerability concept, launched in the second half of the 20th century as a counterweight to the hazard concept [19], has evolved over time to include various dimensions of vulnerability. Nowadays, there are several approaches that encompass multiple dimensions of vulnerability, such as physical, economic, environmental, social, institutional or cultural [16,20]. The final multi-dimensional vulnerability index is calculated by weighting individual dimensions, where each dimension is quantified by weighting specific indicators. Therefore, selecting vulnerability dimensions and appropriate indicators, and assigning their respective weights are critical steps in developing index-based methods.

Presently, there is an increasing tendency to integrate environmental dimensions into index-based vulnerability assessments [14,16,21,22]. In practice, however, vulnerability indices are often assessed by using only two or three dimensions, primarily the social, socioeconomic and/or physical dimensions [23]. Numerous studies [24,25], including the comprehensive reviews by Cho and Chang [26] and Moreira et al. [27], suggested that most authors still give priority (i.e., assign higher weights) to the physical dimension of vulnerability, followed by socioeconomic dimensions [27]. Conversely, lower emphasis is placed on institutional vulnerability [24,28,29], even though this particular dimension has become more significant due to population growth and increasing concentration in flood-prone areas [26]. A negligible number of studies considered cultural vulnerability [30,31].

Assigning weights is another key step in developing index-based methods. According to Moreira et al. [27], Beccari [32] and Papathoma-Köhle [23], many vulnerability studies assign equal weights to different vulnerability dimensions and/or indicators, thereby making them equally important, which does not align with common (stakeholder) perceptions [33]. Generally, weights can be derived by employing data-driven methods, such as regression

analysis, multiple factor analysis, principal component analysis or entropy weighting [34]. Alternatively, weights can be inferred from expert and/or stakeholder elicitation, which may [35–37] or may not [38] be accompanied by multi-criteria decision-making, such as the analytic hierarchy process.

Index-based methods typically have moderate data requirements and can therefore be readily implemented in practice [14]. They can utilize publicly available datasets, such as data on land cover, which contribute to the cost-effectiveness of the vulnerability assessments. More importantly, index-based methods can be applied with heterogeneous data of different types, spatial resolutions and magnitudes, since all the data are aggregated into a single, multi-dimensional vulnerability index. However, it should be noted that the use of low-resolution data may ultimately affect the accuracy of vulnerability assessments. Unlike modeling methods, index-based methods do not require monetization of losses, which further streamlines their usage and reduces uncertainties [17,39]. For instance, physical (buildings and infrastructure) or economic dimensions of vulnerability can be readily expressed in monetary terms; however, monetization of environmental, social and institutional dimensions of vulnerability is exceptionally challenging and can be accompanied by considerable uncertainties [39]. Since index-based methods require no monetization, they can seamlessly integrate these vulnerability dimensions while maintaining moderate data demands.

Index-based methods are scalable and can be applied at different spatial levels, as highlighted by many authors dealing with vulnerability [19,20,35,40–42]. These methods enable cross-regional vulnerability comparisons, as well as their validation against assessments reported in global repositories, such as the "Natural Hazards" database [43]. They also facilitate the evaluation of vulnerability over time, e.g., under different future land-use scenarios, including the implementation of NbSs. Vulnerability assessed by using index-based methods can be readily mapped, thereby facilitating the identification of the most vulnerable areas and the creation of flood risk maps. The vulnerability maps are easily interpreted by stakeholders and can inform decisions about the implementation of risk-reduction measures and sustainable spatial planning under global warming and intensifying natural hazards [44].

The absence of a standardized approach to index-based vulnerability assessment underscores the need to enhance existing methods for more comprehensive yet practically feasible assessments of current and future vulnerability to floods, particularly given the growing role of NbSs and their multifaceted contributions to flood mitigation. Specifically, ex ante vulnerability and, consequently, flood risk assessment represent domains that have remained largely unresolved [14]. To address this gap, we introduce the Multi-dimensional FLOod Vulnerability Index (M-FLOVI) specifically tailored to capture diverse effects of NbSs on vulnerability to floods. M-FLOVI's balanced structure encompasses five key dimensions: namely, physical, economic, environmental, social and institutional. Each dimension is quantified by using a set of indicators carefully selected to serve the M-FLOVI objectives. Some of the M-FLOVI indicators are inherently sensitive to NbS-induced changes (e.g., land cover, creation of protected areas) and, thus, can reflect multidimensional impacts of NbSs on vulnerability. For example, floodplain restoration alters land cover and creates new habitats, both of which are effectively captured by M-FLOVI. In this way, *M-FLOVI systematically integrates NbSs' impacts into post-intervention vulnerability assessments across diverse regions and NbS setups, which represents its core novelty*. A further contribution of M-FLOVI is the first-time application of the self-help capacity indicator in the context of vulnerability assessment. This indicator quantifies the capacity of a community to organize itself and respond during natural disasters [45], and it is purposefully selected to strengthen the assessment of the social and institutional dimensions of vulnerability. Lastly, indicator

selection follows the principle of maximizing the use of information on vulnerability while minimizing data demands and redundancy.

Beyond its novelty, M-FLOVI was designed to provide a link between complex vulnerability concepts and the practical needs of vulnerability and flood risk assessments. Its reliance on widely available datasets makes it broadly applicable and distinguishes it from elaborate indices that depend on extensive surveys measuring, e.g., evacuation knowledge or institutional trust [44]. Its practical applicability was demonstrated within the RECONECT research and development project [46], where M-FLOVI was used to assess vulnerability and flood risk under baseline conditions and various post-intervention scenarios. This paper provides the first comprehensive presentation of M-FLOVI to both the research community and flood risk practitioners, demonstrating its application in the Tamnava River basin in western Serbia, where several large-scale NbSs were proposed to reduce flood risk.

2. The M-FLOVI Index

2.1. Development of M-FLOVI

M-FLOVI encompasses five vulnerability dimensions: namely, physical, economic, environmental, social and institutional. Each dimension consists of several categories calculated from at least one indicator, totaling 13 indicators, as outlined in Table 1 and illustrated in detail in Figures A1–A6 (Appendix A). The categories, which represent an additional layer between the vulnerability dimensions and indicators, were introduced to enhance flexibility and enable more nuanced weighting of the indicators [47]. For instance, if an indicator has to be added or omitted for any reason (e.g., due to highly uncertain or missing data), weight adjustments can be easily made at the level of a category without readjusting the remainder of the weighting scheme. The selection of indicators (Table 1) was guided by international directives [48,49], national government documents [50] and peer-reviewed publications [6,41,51–53], while also being conditioned on data availability [54] and indicator mappability using GIS tools. Throughout, the selection aimed at maximizing the use of information on vulnerability while minimizing data demands and redundancy.

Table 1. M-FLOVI: vulnerability dimensions, categories and indicators, together with their weights. All variables in the table are dimensionless.

Vulnerability Dimension	Dimension Weight (*a*)	Category	Category Weight (*b*)	Indicator	Indicator Weight (*c*)
Physical	0.25	Objects	0.6	Buildings	1.0
		Infrastructure (traffic, communal)	0.4	Roads and railways	0.5
				Bridges	0.5
Economic	0.2	Income	1.0	Population without permanent income	1.0
Environmental	0.15	Natural	0.8	Land Cover (LC)	0.8
				Protected Areas (PA)	0.2
		Anthropogenic environmental	0.2	Landfills	1.0
Social	0.3	Demographic	0.8	Population count	0.6
				Demographic coefficient	0.2
				Self-help capacity	0.2
		Anthropogenic social	0.2	Cultural heritage	1.0
Institutional	0.1	Organizational	1.0	Distance from the main institutions	0.5
				Self-help ratio	0.5

The weights of M-FLOVI were inferred from direct expert and stakeholder elicitation [55–57]. Bearing in mind that vulnerability and, consequently, flood risk assessments should ultimately be accepted by stakeholders and local communities [57], their involvement in the process through co-creation was deemed essential [58]. Therefore, two-round on-site workshops with stakeholders were conducted in the two Serbian pilot cases of the RECONECT project [59]. Individuals and institutions with relevant interest or expertise in NbS were invited by the organizers to participate in the workshops. The participants (21) were representatives of local authorities, water authorities, civil society, politicians, practicing engineers (primarily working in the field of flood management), academia and media. In the first round of the workshops, the participants were asked to anonymously rank certain aspects of NbSs' impacts, which represented the vulnerability dimensions (e.g., social or environmental), from most to least important. Such an approach was adopted for its simplicity. All responses were weighted equally to obtain the overall importance rank of each dimension. These importance ranks, reflecting stakeholders' preferences, were then rescaled to take non-negative values between 0 and 1 with a weight resolution of 0.05, and summing to 1. The resolution of 0.05 was deemed sufficiently fine to reflect stakeholder preferences while avoiding spurious precision, given the uncertainties accompanying the elicitation process. The obtained average ranks, i.e., weights of vulnerability dimensions, were presented to the same group of participants in the second round of workshops for validation. No further adjustments to the initially derived weights were required.

In the first round of workshops, participants clearly prioritized the protection of vulnerable elements against floods (primarily population, then their assets, and protected areas). Therefore, the highest weights were assigned to the physical and social dimensions of vulnerability, whereas the weight assigned to the environmental dimension of vulnerability was lower, as shown in Table 1. Similarly, the participants underscored the greater significance of the environmental dimension compared to the institutional one; thus, the former received a higher weight (Table 1).

The weights assigned to the categories and indicators, on the other hand, were set by the co-author team through an internal elicitation process. The weights of the categories and indicators were determined based on their relative importance from the standpoint of vulnerability to floods. For instance, buildings are considered more vulnerable than traffic infrastructure, since flooding of buildings is often associated with significant loss of assets, and displacement and health risks to residents with long-term implications. Conversely, traffic infrastructure is not associated with moveable assets and is generally designed to withstand some degree of inundation. Steeper slopes of depth-damage curves for buildings than those for traffic infrastructure [60] suggest that relative damages to buildings increase at a higher rate with water depth than those to traffic infrastructure, thereby indicating higher vulnerability. Weight determination also considered relationships among indicators (or categories). For example, natural areas are represented by the land cover indicator; however, a separate indicator "protected areas" was introduced to assign additional vulnerability values to natural areas holding formal protection status. Specifically, the same land cover receives additional value if it falls within a protected area; otherwise, the "protected area" indicator is set to zero and, as such, used further for weighting. As with dimensions, the weights assigned to categories and indicators are expressed as nonnegative values summing to 1 within the parent dimension or category. However, unlike dimensions, categories and indicators received weights with a resolution of 0.1. The coarser resolution is considered sufficient, given that each dimension or category comprises at most three associated items, whereas the five dimensions of M-FLOVI necessitate the finer resolution of 0.05 used at the dimension level.

The final M-FLOVI structure (Table 1) was further benchmarked against typically reported values in the literature [22,24–32,61,62] and, with the dimensions' weights having previously been accepted as credible by the stakeholders (participants), was adopted and used for vulnerability and flood risk assessments across the pilot cases of the RECONECT project [63].

2.2. Calculation of the M-FLOVI Index

2.2.1. Overview

M-FLOVI is calculated from rasterized datasets using GIS software, following the four-step workflow outlined in Figure 1. The first step involves collating the necessary datasets (e.g., land cover, population count) and importing them into a GIS environment. Where needed, datasets are reprojected to a common projection. This step may require adding attributes to the raw (qualitative) dataset, such as types of buildings, if these attributes were not originally included. The second step involves processing these datasets into spatially homogenized rasters carrying numerical values, either retrieved directly from the dataset attributes or assigned nominal values based on the qualitative attributes (e.g., types of buildings). Once processed, each raster is normalized to take values between zero and one. The weighting scheme presented in Table 1 is then applied over these normalized indicator rasters to calculate categories, vulnerability dimensions, and finally M-FLOVI in each pixel. The M-FLOVI values are subsequently classified into four vulnerability classes and mapped to visualize vulnerability to floods in the study area. The study area can represent a river basin, municipality, county, or any other spatial unit, according to the task at hand. The same workflow is followed for assessments of future vulnerability to floods, whereby the projected changes in land cover (including the implementation of an NbS setup) or other anticipated changes (e.g., changes in demographic profile) have to be carefully translated into the corresponding datasets and indicators.

2.2.2. Input Data Processing

The objective of this step is to create rasters at the specified spatial resolution (e.g., 1 m $\times$ 1 m) carrying numerical values needed to calculate M-FLOVI. These numerical values can be obtained in different ways, depending on the dataset. Some rasters (indicators) have measurable, numerical values (e.g., landfill depth), while the values of others can be calculated based on their features (e.g., Euclidean distance from the city center). In many cases, rasters are assigned nominal values based on their qualitative attributes (e.g., building type). It should be noted that nominal values can be assigned with respect to several attributes, such as protected areas or cultural heritage that feature both a protection category and an importance level.

Once assigned numerical values, these datasets have to be harmonized to share the same spatial resolution (e.g., 1 m $\times$ 1 m). This process is also dataset-specific and may include rasterization of vector data according to a relevant attribute (e.g., type of traffic infrastructure, commonly represented by polylines) or disaggregation of coarser rasters to obtain the target resolution. Large-scale indicators necessitate more elaborate downscaling based on proxy data. For example, population count is commonly available at the municipality level but can be downscaled, i.e., spatially distributed according to the locations of residential buildings.

This process is illustrated in Section 3.2, which elaborates the quantification and harmonization of each M-FLOVI indicator in the Tamnava River basin. The process is dataset-specific, and some adjustments are inevitable to integrate locally available data and case-specific conditions into the M-FLOVI workflow.

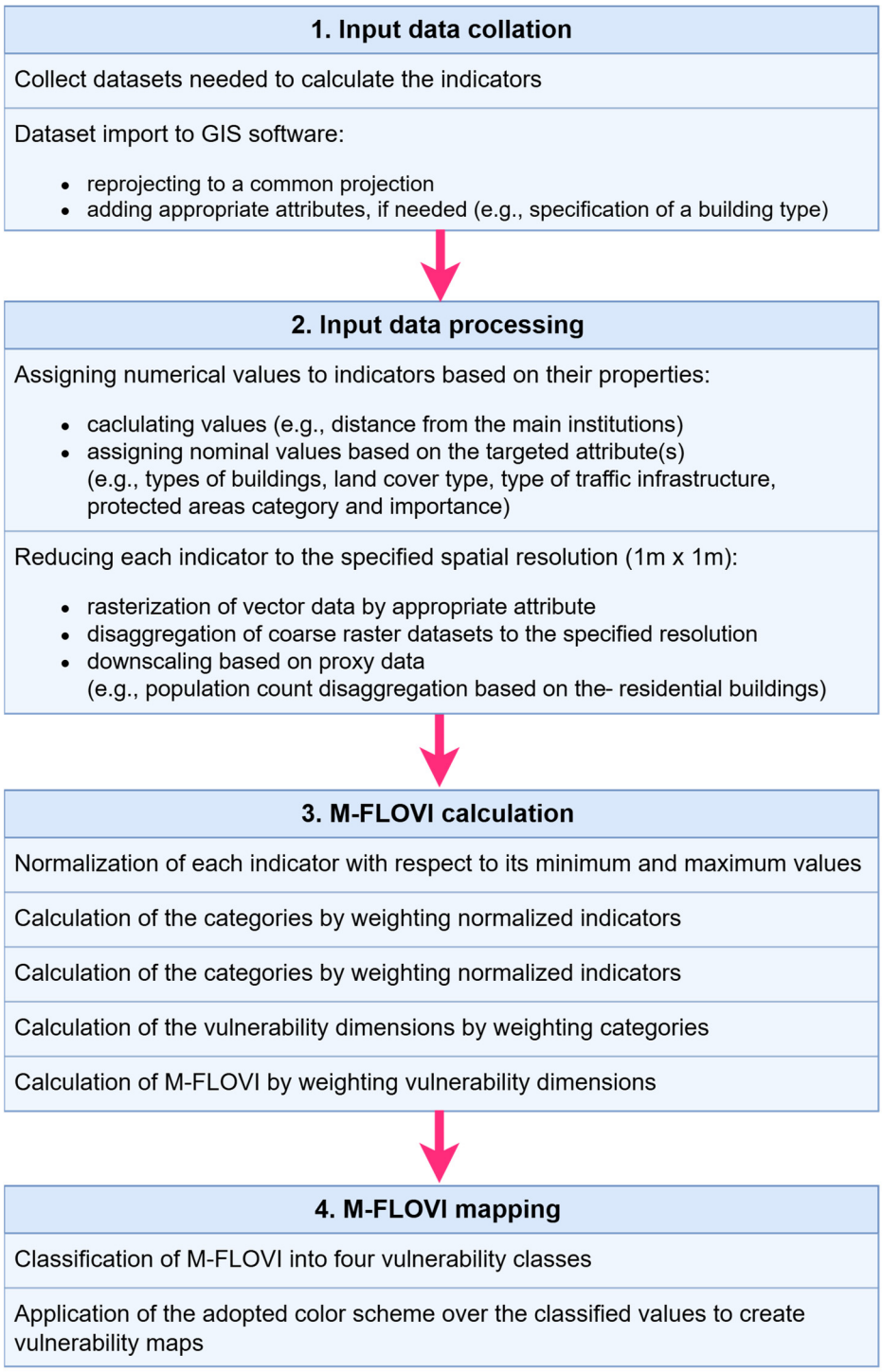

Figure 1. M-FLOVI calculation: a workflow.

2.2.3. The M-FLOVI Calculation

The pre-processed rasters representing indicators (Table 1) considerably vary in their values. To calculate M-FLOVI, the rasters have to be normalized, i.e., rescaled to span the same range. Normalization is conducted for each indicator I separately, with respect to its minimum ($I_{\min}$) and maximum ($I_{\max}$), as follows:

$$I_{\text{norm}} = \begin{cases} \varepsilon, \text{if} I = I_{\min} \\ \frac{(I - I_{\min})}{I_{\max} - I_{\min}}, \text{ otherwise} \end{cases} \quad (1)$$

where ε denotes a small value assigned only to pixels where a normalized indicator equals exactly zero, in order to distinguish them from no-data pixels that are assigned a value of zero by default. The value of ε is kept negligible relative to the normalized scale so that it serves solely as a technical marker, without influencing the final vulnerability scores. In this way, dimensionless normalized indicators (I_{norm}) spanning the range (0, 1] are obtained. The minimum (I_{min}) and maximum values (I_{max}) are set for each indicator separately based on the boundaries of its plausible range. Once set, this range is kept constant across all calculations (e.g., under various scenarios). For example, land cover types are assigned nominal values between one and five (Table A3) under both the baseline and future scenarios, even though the land cover in a given pixel may vary across the scenarios (e.g., due to afforestation).

The vulnerability categories (C) are calculated as the weighted root sum of squares of the normalized indicators (I_{norm}), as follows:

$$C = \sqrt{\sum_{k=1}^{Ni} c_k \cdot I_{norm,k}^2} \quad (2)$$

where c_k stands for the weight of the (normalized) indicator (Table 1) and N_i denotes the number of indicators within category C. The number of indicators N_i varies between one (e.g., objects or income categories) and three (the demographic category within the social dimension of vulnerability).

The vulnerability categories are further used to calculate the vulnerability dimensions D in each pixel, following the same weighting approach:

$$D = \sqrt{\sum_{j=1}^{Nc} b_j \cdot C_j^2} \quad (3)$$

where b_j represents the weight of the jth category (Table 1) and N_c denotes the number of categories in dimension D. As shown in Table 1, either one or two categories are attributed to each vulnerability dimension.

Finally, the M-FLOVI index is calculated in each pixel as the weighted root sum of squares of the five vulnerability dimensions, as follows:

$$\text{M-FLOVI} = \sqrt{\sum_{i=1}^{N_d} a_i \cdot D_i^2} \quad (4)$$

where a_i denotes the weight assigned to the ith vulnerability dimension, while N_d stands for the number of vulnerability dimensions (here: N_d = 5; Table 1).

M-FLOVI is based on the weighted root sum of squares (WRSS), which, by squaring indicator values prior to summation, puts greater emphasis on high values, and thereby on high vulnerability, compared to the weighted arithmetic mean. Specifically, WRSS prevents high vulnerability in one dimension from being compensated by low or moderate vulnerability in others. Since vulnerability assessments are primarily aimed at identifying highly vulnerable areas, WRSS was deemed particularly suitable for M-FLOVI calculations.

2.2.4. M-FLOVI Mapping

The M-FLOVI index ranges between 0 and 1 in each pixel of a study region, and its values were classified into four vulnerability classes: low, moderate, high and very high. The number of classes (4) was adopted to be consistent with the number of flood hazard classes [63,64]. The equal interval classification, which divides the theoretical value range of M-FLOVI (0, 1] into four symmetric intervals, was adopted. Specifically, thresholds of 0.25, 0.50 and 0.75 were set to delineate moderate, high, and very high vulnerability, respectively, whereas values below 0.25 indicate low vulnerability to floods. The equal interval approach

was adopted for two reasons. First, previous research on uncertainties accompanying index-based vulnerability assessments showed that equal interval classification yields vulnerability classes comparable to those obtained by the natural breaks method, which is commonly preferred in the literature [18]. Second, the equal interval classification facilitates communication of vulnerability to the stakeholders, as it is readily interpretable, which, in turn, aids M-FLOVI's broad applicability.

Each pixel was color-coded according to its vulnerability class. We used green to represent low vulnerability, yellow for moderate, and orange and red for high and very high vulnerability, respectively. This color scheme closely resembles the "traffic-light" scheme and provides an intuitive and clear visualization for stakeholders and decision-makers.

2.2.5. Calculation of Future Vulnerability to Floods

The M-FLOVI workflow can be used to calculate future vulnerability to floods. These calculations require adjustment of the input datasets and, consequently, their associated indicators to reflect the future scenario, including NbS implementation. This process is scenario-specific, but in case of NbS implementation, it generally involves changes to the indices within the natural component of the environmental dimension of vulnerability (land cover and protected area). NbS implementation can also create new green jobs in some cases [58], thereby reducing the share of population without permanent income, an indicator within the economic dimension of vulnerability. Nevertheless, capturing all potential effects of NbSs is not a straightforward task, and some effects, such as the creation of educational opportunities, cannot be captured by M-FLOVI due to the absence of suitable indicators.

In addition to NbSs, future vulnerability assessments should account for future changes in population size and demographic profile, as well as projected changes in land cover and commercial activities, all of which can be captured by the M-FLOVI indicators.

3. Application of M-FLOVI in the Tamnava River Basin in Serbia

The M-FLOVI index was calculated in the Tamnava River basin in the west of Serbia (Figure 2), where an NbS setup comprising several different measures was proposed to reduce flood risk (Figure 3). To this end, a suite of indicators listed in Table 1 was quantified and weighted to calculate categories, five vulnerability dimensions, and lastly the M-FLOVI index under the baseline and future conditions. The Tamnava River basin and the proposed NbS setup are presented in Section 3.1, whereas Section 3.2 elaborates on the calculation of M-FLOVI in this basin.

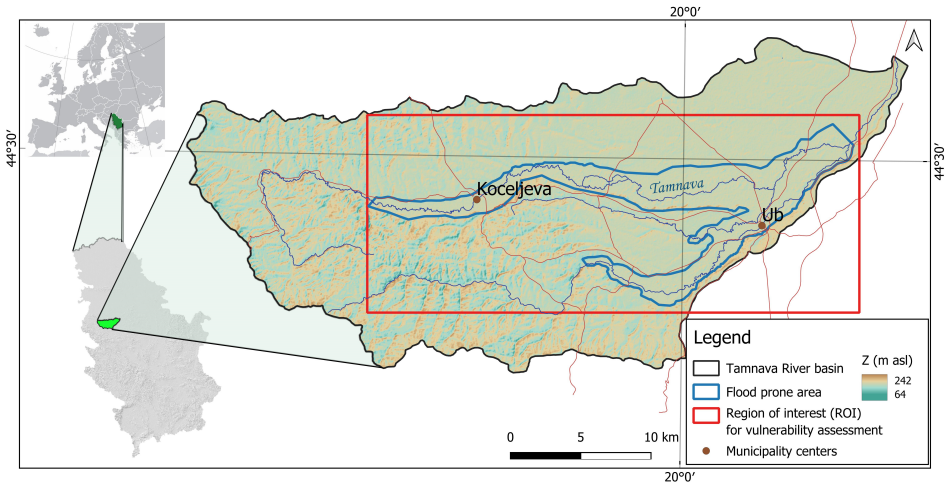

Figure 2. Location of Tamnava River basin with marked region of interest (ROI) where the flood vulnerability assessment was carried out.

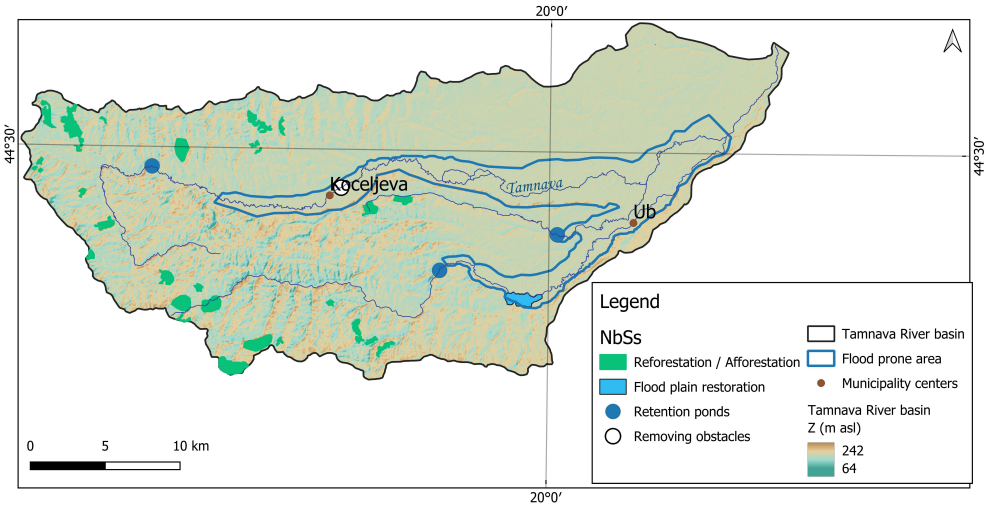

Figure 3. The proposed NbSs in the Tamnava River basin.

3.1. The Tamnava River Basin

The Tamnava River basin, covering an area of 726 km^2 in western Serbia, flows west-to-east towards its confluence with the Kolubara River, which is the southernmost downstream right tributary of the Sava River. Both plains and hilly areas are represented in the basin (Figures 2 and 3). Such orography is reflected in floods: torrential floods occur in the headwater parts of the basin, while fluvial floods hit its mid-parts and downstream lowland. The basin is prone to frequent flooding: in particular, the riparian areas along the Tamnava River and its main tributary, the Ub River, were hit by severe floods in 1999, 2006, 2009 and 2014, resulting in substantial losses, injuries, and even fatalities [59,65,66], also accompanied by population displacement [67]. Due to the local lithology, which includes quartz sandstones; slightly metamorphosed argillites and phyllites in the headwater parts; and conglomerates, sands and clays further in the middle and lower parts of the basin [68], floods are commonly accompanied by intensive erosion.

Flood vulnerability, along with the local population, is concentrated in the municipalities of Koceljeva and Ub (Figure 2), whereas agricultural areas predominate over the built-up areas in the remainder of the basin. The existing flood protection infrastructure relies primarily on embankments along the Tamnava and Ub Rivers within the two urban centers, and downstream of Ub extending to the Kolubara River confluence. However, this infrastructure is not effective enough, so the local and national authorities consider complementing it with NbSs [12,63,69]. To this end, the effectiveness of an NbS setup in the Tamnava River basin is evaluated as part of the RECONECT project [63]. The proposed setup includes (1) three retention ponds (Pambukovica, Ćukovina and Gračica); (2) afforestation, mainly in the basin's headwaters; (3) floodplain restoration by restoring the Dokmir fishpond on the Ub River; and (4) removal of obstacles, i.e., widening of the bridge opening immediately downstream of Koceljeva (Figure 3). In addition to the NbSs, the implementation of a photovoltaic power plant can be expected in the future according to spatial plans, all of which can affect future vulnerability to floods.

3.2. Calculation of the M-FLOVI Index in the Tamnava River Basin

3.2.1. Input Data Collation and Processing

The M-FLOVI index was calculated in the Tamnava River basin at 1 m × 1 m spatial resolution and in UTM N34 projection. To make the calculations computationally tractable, the analyses were limited to a region of interest (ROI), which was defined as a bounding box covering an area inundated by a 1000-year water level with a freeboard of 0.5 m (Figure 2). The water level of a 1000-year flood was obtained from the unsteady 1D–2D hydrodynamic

simulations in HEC-RAS [70], which was forced by flood hydrographs simulated by the semi-distributed rainfall-runoff model 3DNet-Catch [71]. These modelling efforts were part of a flood risk assessment conducted within the RECONECT project [63], but the resulting inundation extent was also used to delineate the ROI for the vulnerability assessments.

The resulting ROI of the Tamnava River basin covers an area of over 490 km^2 and contains about 6000 buildings, 65% of which are residential, while the share of agricultural and commercial buildings is smaller. The ROI also includes 35 km of Category I and II roads, classified according to the national road classification [72], and 35 bridges. The ROI administratively belongs to the municipalities of Ub and Koceljeva. According to the 2022 Census [73], 8430 people live in the ROI, most of whom are concentrated in urban centers and along major roads. The demographic profile shows a predominance of younger (under 15) and elderly residents (over 64). According to [73], on average, 45% of Ub's population lives without permanent income, and this figure can reach 80% in certain settlements of this municipality. In Koceljeva, this share amounts to 40%. These values suggest a high level of social and economic vulnerability of the local population. The basin is primarily agricultural, with prevailing arable land [74]. There are 19 landfills in the basin, five of which are situated within the ROI. With the exception of one sanitary landfill, the remainder are illegal dumping sites [75], which significantly increase the environmental dimension of vulnerability. Under the baseline conditions, there are no protected areas in the Tamnava River basin [76], but the basin hosts 17 immovable cultural properties (IMPs), five of which (one archaeological site and four monuments of culture) are located in the ROI and amplify the social dimension of vulnerability to floods.

Most of the required datasets were obtained from national or global repositories (Table 2) and collated in QGIS [77]. Buildings and roads in the ROI were digitized from high-resolution Google Maps (2024) imagery [78] by the authors [69,72]. Positional errors in Google Maps range between 1 m and 10 m in urban zones and between 5 m and 10 m in rural areas [79]. A maximum zoom level was applied throughout. The resulting file was validated in QGIS by overlaying it with the OpenStreetMap dataset, which showed positional differences of 0–5 m [80].

Table 2. Data and sources used to calculate M-FLOVI in the Tamnava River basin. Please note that spatial resolution refers to the original (raw) dataset.

Indicator	Data Source	Data Type	Spatial Resolution	Attribute (Units)
Buildings	Google maps [78] and Open Street services 2024 [80]	vector—polygon	1 m	Building type (-)
Roads and railways		vector—polyline	1 m	Road category (-)
Bridges		vector—polyline	1 m	-
Population without permanent income	Census data 2022 [73]	vector—polygon	settlement-level	Percentage (%)
Land Cover (LC)	Corine 2018 [74]	raster	100 m × 100 m	CLC 2018 code
Protected Areas (PA)	Institute for Nature Protection of Serbia [81]	vector—polygon	1 m	Protection category (-) and importance (-)
Landfills	Serbian Environmental Protection Agency [75]	vector—point	1 m	Landfill depth (m)
Population count	Census data 2022 [73]	vector—polygon	settlement-level	Number of people
Demographic coefficient	Census data 2022 [73]	vector—polygon	settlement-level	Total dependency ratio (-)

Table 2. *Cont.*

Indicator	Data Source	Data Type	Spatial Resolution	Attribute (Units)
The self-help capacity	Census data 2022 [73]	vector—polygon	settlement-level	Number of people
Cultural heritage	Institute for the Protection of Cultural Monuments of Serbia [82]	vector—polygon	1 m	Protection category (-) and importance (-)
Distance from main institutions	Calculated by the authors using QGIS [77]	raster	1 m	Distance (m)
The self-help ratio	Census data 2022 [73]	vector—polygon	settlement-level	Relative value (-)

Table 2 lists the data sources used for indicator quantification in the Tamnava River basin. These datasets are generally available, and practitioners or researchers aiming at applying M-FLOVI elsewhere can readily use the same data sources or identify locally available equivalents. As for the Tamnava case, the input datasets varied considerably in spatial resolution: for example, buildings, transportation infrastructure and cultural heritage data were available at a rather fine resolution of 1 m. Population data from the 2022 Census [73] were disaggregated to 1 m resolution according to digitized residential buildings. On the other hand, economic and demographic data (e.g., the demographic coefficient, self-help capacity), as well as institutional data were available only at the settlement level. Therefore, these datasets had to be disaggregated or downscaled to 1 m $\times$ 1 m to enable M-FLOVI calculations. Spatial homogenization and the assignment of numerical values to each indicator are described in the remainder of this subsection.

1. **Physical vulnerability**

Buildings. Fourteen types of buildings were identified in the Tamnava River basin (Table A1). Each type was assigned a nominal value for vulnerability assessment, with higher nominal values indicating higher vulnerability to floods. For example, buildings serving governmental, educational or commercial purposes were assigned the highest nominal value (5), reflecting their high social and economic significance and the difficulties of replacing them after a flood event. Industrial and institutional buildings were assigned intermediate values. Residential buildings were assigned various nominal values. Specifically, single-story ground floor-only houses were assigned higher nominal values than other residential building types, since they offer no possibility to evacuate occupants or move assets to upper floor(s) that would otherwise remain beyond flood reach. Therefore, this building type is considered more vulnerable than its multi-story counterparts. The lowest nominal values were assigned to the agricultural and auxiliary buildings, as well as transportation hubs, which are generally considered structures without significant movable content. The 14 types of buildings and their nominal values are presented in Table A1 of Appendix B.

Roads and railways. According to the national road classification [72], first-order national roads (subcategories IA and IB), as well as second-order roads (subcategories IIA and IIB) were identified in the Tamnava River basin. Nominal values were assigned based on road category, reflecting the relative economic and functional significance of each road type. Highways received the highest nominal value (5), as they represent the highest-order infrastructure with the greatest replacement cost and potential for traffic disruption. Other types of roads gradually received lower nominal values, proportional to their functional classification (Table A2). Railways were assigned the highest nominal value (5) given their economic significance, and the complexity and cost of their repair. However, no railway infrastructure was identified in the ROI.

Bridges were extracted from the road network rasters. To quantify this indicator, pixels representing bridges were assigned a value of 1, while the remaining road pixels were assigned a value of 0. Since the indicator only takes values between zero and one, no normalization was required.

These indicators were calculated only within pixels that represent buildings, traffic infrastructure, or bridges. The remaining pixels were assigned values of zero, i.e., they were considered no-data pixels.

2. **Economic vulnerability**

Population without permanent income was expressed as the percentage of the settlement population without permanent income. The data were then rasterized at the settlement level, with all pixels within a given settlement receiving the same value of this indicator.

3. **Environmental vulnerability**

Land cover data were grouped into five classes, according to the CORINE land cover Level 1 classification [74], and each class was assigned a nominal value as presented in Table A3 (Appendix B). The highest nominal value (5) was assigned to artificial surfaces, which were deemed most vulnerable due to population exposure, high density of assets, and consequently higher market value, followed by agricultural areas. Pastures were assigned a slightly lower nominal value than agricultural areas, reflecting their comparatively lower economic productivity. Forests and semi-natural areas were assigned a lower nominal value than agricultural land, as they are generally more resilient to flooding and are not associated with crop losses. The lowest nominal value (1) was assigned to water bodies and wetlands.

Protected areas were classified into five classes according to the category of protection (as per Table A4 of Appendix B), and further stratified by protection importance (three levels; Table A6), both of which determine the rank of a protected area, as prescribed by the Law on Nature Protection [83]. Each protected area was assigned two nominal values according to its category and importance level. The final nominal value of a protected area was calculated as the weighted root sum of squares (WRSS), where both nominal values were assigned the same weight of 0.5. Information on protection categories and importance levels can be obtained from the Law on Nature Protection in the Republic of Serbia [83].

Landfills were represented by their depths, which were considered indicative of environmental vulnerability, as landfill depth reflects the amount of waste stored, and thus the potential for flood-borne contamination. Landfill depths were obtained from the Serbian Environmental Protection Agency, which maps all landfills, including illegal dumping sites. The landfill database is updated regularly based on information acquired through field surveys [75].

4. **Social vulnerability**

Population count. These data were available only at the settlement level and were downscaled to be suitable for pixel-level vulnerability assessments. To this end, the total population of a settlement was divided by the number of residential buildings to estimate the mean household size. This ratio was then redistributed proportionally to the floor area of each residential building to obtain the number of residents per pixel within each residential footprint, thereby downscaling the population to the pixel level. It should be noted that this downscaling procedure does not improve the accuracy of the source data but serves solely to enable pixel-based calculations.

The demographic coefficient was represented by the total dependency ratio (*TDR*), which was calculated as the total number of young (under 15; $N < 15$) and elderly residents (over 64; $N > 64$), divided by the working-age population (15–64; $N_{15–64}$), as follows:

$$TDR = (N_{<15} + N_{>64})/(N_{15–64}) \quad (5)$$

This indicator was rasterized at the settlement level, with all pixels within a given settlement receiving the same value.

The self-help capacity (termed the self-help coefficient in [45]) represents the number of people who can be mobilized and can potentially assist others during natural disasters. This indicator was, therefore, considered particularly suited to vulnerability assessments and preferred over other demographic indicators, such as the age structure or the demographic coefficient that reflects population vulnerability (fragility). The indicator was calculated at the settlement level by weighting population count within each age group by predefined coefficients proposed by [45]. It was further rasterized, with all pixels within a given settlement receiving the same value. Since higher values of this indicator correspond to lower vulnerability to floods (and other natural disasters), the inverse of its normalized value was used in vulnerability assessment.

Cultural heritage was represented by immovable cultural properties (IMPs), classified into five classes based on both the protection category of each IMP and protection importance (three levels) [82]. Accordingly, two nominal values were assigned to each IMP and then averaged to quantify this indicator at the pixel level, following the same approach as for protected areas. The assigned nominal values are presented in Tables A5 and A6 of Appendix B.

5. Institutional vulnerability

Distance from main institutions. This indicator was represented by the Euclidean distance between each pixel within the ROI and the center of the nearest town, where key emergency institutions (police, fire services, hospitals and emergency response units) are typically located. Greater distances imply longer response times and therefore higher vulnerability.

The self-help ratio is defined as the ratio of the self-help capacity to the total settlement population and reflects how effectively local communities may be organized in an emergency to form a group large enough to provide assistance to others [45]. Higher values of this ratio (close to 1) indicate less vulnerable communities. Therefore, the inverse of the self-help ratio was rasterized to the pixel level for calculating the institutional dimension of vulnerability.

The protocol for quantification of indicators at the pixel level is consolidated in Table 3. Together with the data sources provided in Table 2, Table 3 provides a sufficient basis for reproducing M-FLOVI calculations.

Table 3. Protocol for quantification of the M-FLOVI indicators in the Tamnava River basin: a summary.

Indicator	Value Estimation
Buildings	A nominal value is assigned to each pixel representing buildings, depending on the building type (Appendix B: Table A1).
Roads and railways	A nominal value is assigned to each pixel representing traffic infrastructure, depending on its type (Appendix B: Table A2).
Bridges	A value of 1 was assigned to pixels encompassing bridges, while the remaining pixels received a value of 0.

Table 3. *Cont.*

Indicator	Value Estimation
Population without permanent income	The percentage of population without permanent income, disaggregated to a pixel level.
Land Cover (LC)	A nominal value is assigned depending on the specific land cover (Appendix B: Table A3)
Protected Areas (PA)	A nominal value is assigned to each pixel representing a protected area, depending on the category and level of protection (Appendix B: Table A4)
Landfills	Landfill depth obtained from the Serbian Environmental Protection Agency [75].
Population count	Total population in a settlement, downscaled at a pixel level according to the residential building footprints.
The demographic coefficient	Represented by the total dependency ratio (*TDR*), which is calculated by dividing the number of people under 14 15 ($N_{<15}$) and over 64 ($N_{>64}$), by the number of working-age people ($N_{15–64}$): $TDR = (N_{<15} + N_{>64})/(N_{15–64})$
The self-help capacity	Number of people per settlement who can assist others in emergencies, disaggregated to the pixel level. The inverse of this indicator is used in the calculations.
Cultural heritage	A nominal value assigned depending on the category and level of protection (Appendix B: Table A5)
Distance from main institutions	Euclidean distance between a pixel and the nearest municipality center.
The self-help ratio	Ratio between the self-help capacity and the total population of a settlement, disaggregated to the pixel level.

3.2.2. The M-FLOVI Calculations Under the Baseline and Future Scenarios

After processing the input data, M-FLOVI was calculated by applying the weighting scheme elaborated in Section 2. Specifically, the weighting scheme was applied to the normalized indicators in each pixel of the region of interest (ROI) to calculate the categories (Equation (2)), vulnerability dimensions (Equation (3)), and lastly M-FLOVI (Equation (4)). The M-FLOVI values were then classified into four vulnerability classes (low, moderate, high, and very high) and visualized by using the selected color scheme described in Section 2.2, where green and red indicate low and very high vulnerability, respectively.

In addition to baseline conditions, the M-FLOVI index was calculated under two alternative future scenarios (Table 4). The first scenario (denoted S0, "without NbSs") included only projected land cover change (implementation of a photovoltaic power plant), as defined in the spatial plans, while the second scenario (denoted S1, "with NbSs") additionally included the proposed NbS setup in the Tamnava River basin (Section 3.1). In all scenarios, the M-FLOVI was calculated following the same protocol, but with scenario-specific indicator values.

For example, under the baseline conditions, Dokmir has no protection status, meaning that the affected pixels were treated as no-data pixels in terms of the protected areas indicator. Concerning land cover, Dokmir represents a wetland and thus received the lowest nominal value of 1 according to Table A3. After applying Equation (1) (Section 2.2), the normalized value of the land cover indicator of ε was obtained, thereby distinguishing the affected pixels from the no-data pixels. Here, a value of ε = 0.00025 was adopted as 1% of the interval width (0.25; Section 2.2). The natural category under the baseline conditions was, therefore, calculated by multiplying the normalized land cover indicator by its weight of 0.8 (as per Table 1), whereas the protected area indicator was treated as no-data pixels, as follows:

$$C_{\text{natural, baseline}} = \sqrt{0.8 \cdot (0.00025)^2 + 0.2 \cdot 0^2} = 0.00022 \quad (6)$$

The Dokmir fishpond is expected to receive protected habitat status of the third level of protection (i.e., local habitat status) following its restoration under scenario S1, which is the status that it previously held [84]. To accommodate floodplain restoration (i.e., the restoration of the Dokmir fishpond), the affected pixels were assigned nominal values of 1 according to both the protected area category (Table A4) and importance (Table A6). After applying the weighted root sum of squares equation, these two values yield the overall nominal indicator value of 1. Considering that a protected area can receive nominal values between 1 and 5 and between 1 and 3 according to its category and importance, respectively, the minimum (I_{min}) and maximum indicator values (I_{max}) amount to 1 and 4.12, respectively. Normalization of this indicator according to Equation (1) yields a value of ε. Since the Dokmir fishpond retains the same land cover code and the normalized value of this indicator as under the baseline conditions, the natural category of these pixels was calculated as follows:

$$C_{\text{natural, S1}} = \sqrt{0.8 \cdot (0.000025)^2 + 0.2 \cdot (0.00025)^2} = 0.00025 \quad (7)$$

The increase in the natural category under S1 is reflected in both the environmental vulnerability dimension and the final M-FLOVI value.

Table 4. Summary of the scenarios under which M-FLOVI is calculated.

Scenario	Comment
Baseline	○ Current buildings, infrastructure and land cover in the basin ○ No NbSs implemented in the ROI
Future state without NbSs (S0)	○ Implementation of the photovoltaic power plant accompanied by land cover change (25.8 ha) ○ No NbSs implemented in the ROI
Future state with NbSs (S1)	○ Implementation of the photovoltaic power plant (25.8 ha) ○ Proposed NbSs implemented in the basin ■ three retention ponds, with water surface of 210 ha in the ROI ■ afforestation of 392 ha, of which 291 ha in the ROI ■ floodplain restoration (158 ha) ■ removal of obstacles (i.e., widening of the bridge opening)

The land cover change due to the photovoltaic power plant was accounted for by updating the land cover and buildings indicators in the affected pixels. Specifically, land cover was assigned the highest nominal value (5) reserved for artificial surfaces (Table A3), while the associated buildings received a nominal value of 4. This value corresponds to energy facilities, which can contain valuable equipment, but do not involve permanent human occupancy or high asset density characteristic of commercial or governmental buildings (similarly to light industrial buildings; Table A1).

The projected changes can potentially create new jobs, including green jobs, such as those associated with ecotourism and habitat management in the restored Dokmir fishpond, which may ultimately affect the population without permanent income indicator within the economic dimension of vulnerability. However, quantification of the resulting change in this indicator is inherently uncertain, as it depends on the scale of job creation and local labor market conditions, neither of which can be reliably estimated from the available data. This indicator was, therefore, held constant across the scenarios, as adjusting it based on

assumptions about socioeconomic tendencies was deemed to introduce greater uncertainty than the simplification itself. The same assumption was adopted for landfills, which may either spread or be remediated with equal likelihood, as well as for the demographic-related indicators. The distance from the main centers is expected to remain unchanged in the foreseeable future, since spatial plans indicate no planned development of new towns in the Tamnava River basin. Therefore, the economic, social and institutional dimensions of vulnerability remain the same across the scenarios.

4. Results

The M-FLOVI values indicate predominantly moderate vulnerability to floods in the Tamnava River basin under baseline conditions, with a mean value of 0.324 (Table A7), reflected in the prevailing yellow shading in Figure 4. Slightly over 15% of the ROI shows low vulnerability (Table A8), as also indicated by the limited green shading in Figure 4. High vulnerability is concentrated in the centers of Ub and Koceljeva municipalities due to the concentration of built-up areas and demographic characteristics. High vulnerability is also detected in the northeast of Ub, attributable to the presence of vulnerable, economically disadvantaged groups (Figures A8 and A10 of Appendix C). Together, high and very high vulnerability account for less than 1% of the ROI (368 ha and 1 ha, respectively), with the highest M-FLOVI value of 0.777 (Table A7) marginally exceeding the very high vulnerability threshold of 0.75.

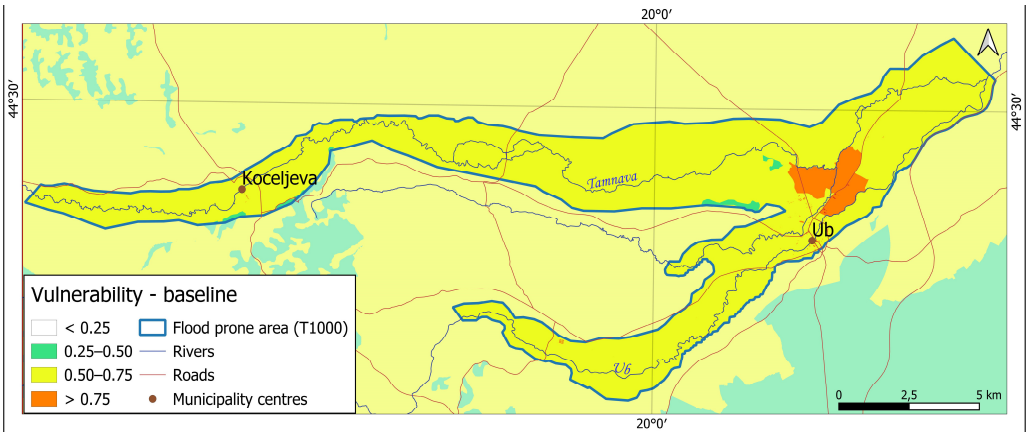

Figure 4. Vulnerability to floods in the Tamnava River basin under baseline conditions. The flood prone area is indicated by more intense color tones than the remainder of the ROI.

The maps showing the five dimensions of vulnerability (physical, economic, environmental, social and institutional) are provided in Appendix C (Figures A7–A11) and summarized in Figure 5a. Concerning *the physical vulnerability dimension*, the vast majority of the ROI represents no-data pixels (i.e., pixels that do not contain buildings or traffic infrastructure), as indicated by the grey areas in Figure A7. Vulnerability classes appear discrete on the map, since they refer to digitized individual buildings and linear traffic infrastructure. Only 251.4 ha of the ROI represent either buildings or traffic infrastructure, of which 55.8% is of low and 35.2% is of moderate physical vulnerability (Figure 5c). High and very high physical vulnerability represent 4.8% and 4.1% of the area under buildings or traffic infrastructure, becoming negligible (i.e., lower than 1%; Table A8) when considered relative to the entire ROI area (Figure 5a). As for the *economic dimension*, areas with high and very high vulnerability cover approximately 2% of the ROI (Table A8). Low and moderate economic vulnerability account for 64.9% and 33.2% of the ROI, respectively, which translates to the prevalence of green and yellow shades in Figure A8.

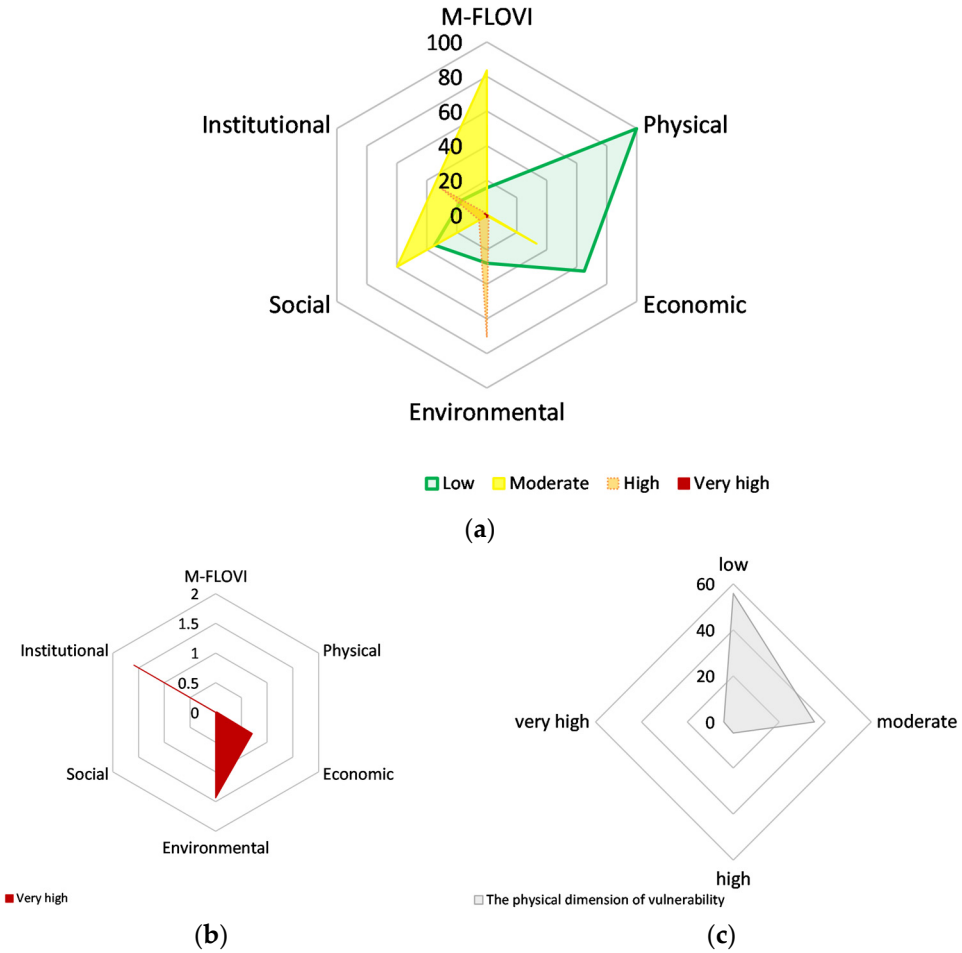

Figure 5. (**a**) The M-FLOVI vulnerability dimensions in the Tamnava River basin under baseline conditions presented across four vulnerability classes and (**b**) very high vulnerability as the percentage of total area of the ROI, and (**c**) the physical dimension of vulnerability as a percentage of area under buildings or traffic infrastructure.

High *environmental vulnerability* predominates, covering slightly over 70% of the ROI (Table A8; Figure 5a), with very high values in the urban areas (Figure A9). Less than one third of the ROI exhibits low or moderate environmental vulnerability (27.9% and 0.4%, respectively; Table A8 and Figure 5a). Moderate *social vulnerability* preponderates in the study area (nearly 60% of the ROI), followed by low vulnerability (34.9%; Table A8). High social vulnerability (5.3% of the ROI; Table A8) can be found in areas with a prevalent elderly population and in areas inhabited by vulnerable groups (Figure A10). Conversely, the high population count, low demographic coefficient and high self-help capacity in the urban centers resulted in low social vulnerability in these areas. Since the *institutional dimension of vulnerability* is based on the Euclidean distance to the nearest town center, values increase with distance from Koceljeva and Ub (Figure A11 of Appendix C). The slight departures from "concentric-ring" patterns in Figure A11 are due to the self-help ratio, which also shapes the institutional dimension of vulnerability. The vast majority of the ROI exhibits moderate (51.2%) and high vulnerability (30.3%), whereas very high institutional vulnerability is present in less than 2% of the study area (Figure 5b; Table A8).

The projected change in the Tamnava River basin implies the implementation of a photovoltaic power plant in an agricultural area within the ROI (Section 3.1). These changes were analyzed under the S0 scenario ("without NbSs"), while the S1 scenario additionally includes the proposed NbS setup, which further alters land cover in the ROI, and creates a protected bird habitat (Section 3.1). Consequently, changes in the

physical and environmental dimensions of vulnerability, and therefore in the M-FLOVI values, are obtained under the two future scenarios (Table A8). Economic, social and institutional dimensions remain the same as under the baseline conditions (Table A8), since the future changes in the ROI do not affect any of their constituent indicators. The population without permanent income indicator was kept constant across all scenarios (as elaborated in Section 3.2), thereby resulting in unchanged economic dimension of vulnerability (Table A8).

The construction of a new photovoltaic power plant drives three key changes to vulnerability to floods across the ROI. Specifically, it increases the physical vulnerability of no-data to high across 25.8 ha (i.e., 0.06%) of the ROI relative to the baseline conditions (Figure A12, Table A8). It also increases the environmental vulnerability class from high to very high in the same area due to land cover change (Figure A13; Table A8). Lastly, these changes are reflected in the M-FLOVI classes (Figure 6), which increase from moderate to high in the affected area (Table A8); however, the change to the mean M-FLOVI value is negligible (Table A7). The changes to M-FLOVI classes under the future S0 scenario ("without NbSs") are clearly outlined in Figures 7 and A15.

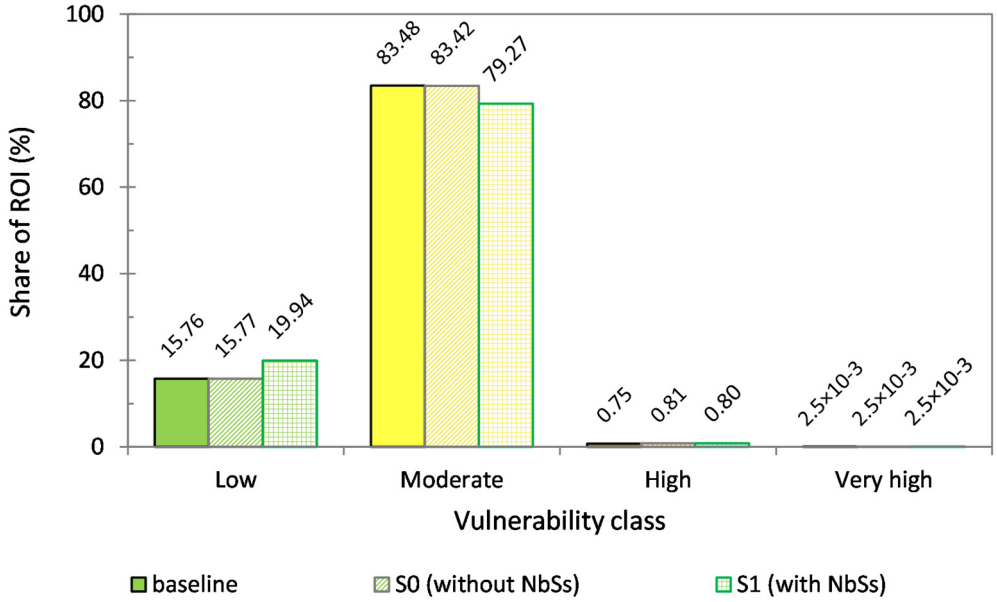

Figure 6. Share of four vulnerability classes in the region of interest under baseline conditions and two future scenarios: S0—without NbSs, and S1—with NbSs.

On the other hand, the implementation of NbSs under the S1 scenario reduces vulnerability, as reflected in the mean M-FLOVI value (Table A7). This decrease is caused by changes in land cover (highlighted in Figures 8 and A16). Specifically, the conversion of agricultural land to water bodies (retention ponds and floodplain restoration) or forested land (afforestation) decreases the environmental vulnerability, as these land cover types are considered less vulnerable than agricultural land. High vulnerability in 0.9% of the ROI transitions to either low (0.61%) or moderate (0.29%), whereas 0.05% increases to very high vulnerability (Figure 6; Table A8). The locations of these changes are indicated by green boxes in Figures A14 and A16 of Appendix C. In contrast, floodplain restoration (i.e., restoration of the Dokmir fishpond, indicated by a green box in the bottom of Figure A14) locally increases the environmental vulnerability. The fishpond is expected to provide a bird habitat and become a protected area under S1, which increases the natural category and consequently the environmental vulnerability. Overall, the proposed NbS setup generally makes localized changes in the M-FLOVI values across the ROI. For instance, even though

floodplain restoration affects the environmental vulnerability, the resulting M-FLOVI class remains moderate, consistent with the baseline conditions.

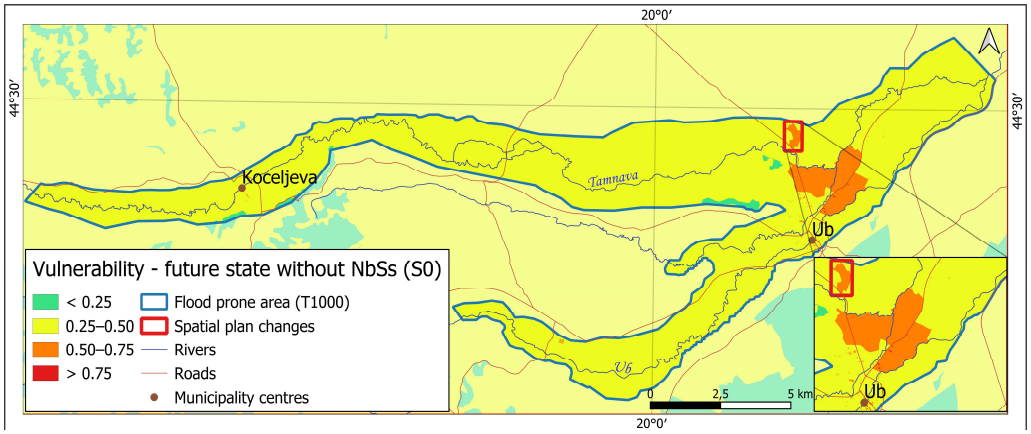

Figure 7. Vulnerability to floods in the Tamnava River basin under the future S0 scenario ("without NbSs"). Red box indicates increased vulnerability due to the projected photovoltaic power plant. The flood prone area is shown by more intense color tones than the remainder of the region of interest (ROI).

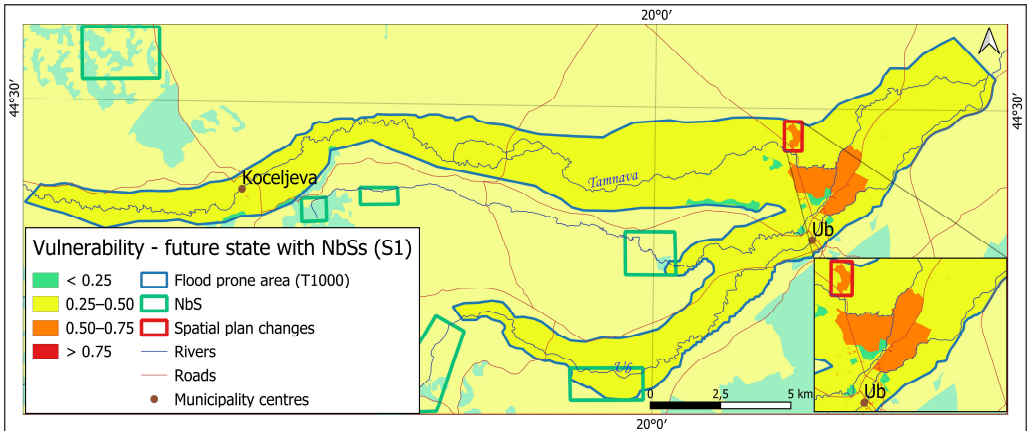

Figure 8. Vulnerability to floods in the Tamnava River basin under the future S1 scenario ("with NbSs"). Green boxes indicate areas of reduced vulnerability due to NbS implementation, while red box indicates increased vulnerability due to the projected photovoltaic power plant. The flood prone area is shown by more intense color tones than the remainder of the region of interest (ROI).

5. Discussion

5.1. Vulnerability to Floods Under the Baseline and Future Conditions

This paper presents a novel Multi-dimensional FLOod Vulnerability Index (M-FLOVI) that is calculated from five vulnerability dimensions: namely, physical, economic, environmental, social and institutional. The index development was guided by current trends to comprehensively quantify vulnerability and to account for the impacts of NbSs on post-intervention vulnerability to floods [14,16,27–29,31,51–54]. In this paper, the M-FLOVI values were calculated in a region of interest (ROI) within the Tamnava River basin under baseline conditions, and under two future scenarios. One future scenario (S0) implies the development of a photovoltaic power plant, leading to a change in land cover (i.e., conversion of agricultural land to artificial areas), as defined in the available spatial plans. The other scenario (S1) additionally implies the implementation of a proposed NbS setup comprising three retention ponds, afforestation, floodplain restoration, and removal of obstacles (Figure 3). Except for the removal of obstacles, these NbSs alter land cover,

whereas floodplain restoration (i.e., restoration of the Dokmir fishpond), which is expected to receive protected area status under S1, additionally affects the protected area indicator within the environmental vulnerability dimension.

Under the baseline conditions, moderate vulnerability to floods prevails in the ROI of the Tamnava River basin, whereas a region populated by socially vulnerable groups shows high or very high vulnerability. The assessed vulnerability to floods in Koceljeva and Ub municipalities largely corresponds to the findings presented by Kovačević-Majkić et al. [41], who assessed vulnerability at the municipality level in Serbia over a 32-year period (1971–2002). Higher social vulnerability to floods in the municipality of Ub was also reported by Panić [85], thereby corroborating higher M-FLOVI values in this municipality obtained in this study. Moreover, the social and economic dimensions of vulnerability assessed in this study under the baseline conditions closely align with the results obtained in three projects carried out in this region: namely, *Danube Flood Risk* funded by ICPDR, *SoFPAS in Serbia* funded by IPA2007 and *Flood Recovery Serbia* funded by IPA 2014–2020 [86]. Finally, the devastating floods that hit the Tamnava River basin in May 2014 caused the most severe consequences in urban centers [59,65,66], i.e., in the most vulnerable areas indicated by M-FLOVI. These validation results suggest that the proposed method can yield realistic vulnerability assessments with reasonable data and computational demands.

The M-FLOVI index was also used to assess future vulnerability to floods under two alternative scenarios. The index effectively captured an increase in vulnerability across 25.8 ha due to the photovoltaic power plant implementation under the S0 scenario, which implies conversion of agricultural land into more vulnerable artificial areas and implementation of energy use buildings. The index also captured a decrease in overall vulnerability due to the implementation of the NbSs (afforestation, retention ponds and floodplain restoration) under the S1 scenario. These NbSs imply land cover conversion to less vulnerable forested areas and wetlands. Most importantly, the index captured a localized increase in environmental vulnerability at the location of the Dokmir fishpond (floodplain restoration), which is expected to become a protected area of the 3rd protection level under the S1 scenario. These results clearly suggest that M-FLOVI can comprehensively capture various NbSs' impact on future vulnerability to floods, and can, therefore, enable plausible assessments under various scenarios.

The effectiveness of NbSs is typically evaluated based on their ability to reduce flood hazard and/or flood risk, as well as the co-benefits they can provide [39]. However, we propose considering vulnerability reduction as an additional criterion in the multi-criteria evaluation of an NbS setup and including the impact on vulnerability to floods in operational decision-making in spatial planning and water management sectors. The vulnerability maps reflect differences among spatial units within the study area and can thus assist stakeholders and decision-makers in identifying the most vulnerable areas under each future scenario, enabling informed decisions about flood risk management (FRM) options, as well as their prioritization [69]. In practical terms, M-FLOVI outputs can be directly integrated into spatial planning instruments, such as municipal flood risk management plans and land use plans, to guide the allocation of NbS measures towards areas of highest vulnerability. For instance, vulnerability maps produced under different future scenarios can inform spatial planning decisions by identifying areas where projected land use changes would increase vulnerability and where targeted NbS interventions would be most effective in offsetting these increases. Furthermore, the scenario-based structure of M-FLOVI allows planners and water managers to compare the vulnerability implications of alternative development pathways before committing to irreversible land use decisions, thereby supporting proactive rather than reactive flood risk governance. The proposed NbS setup in the Tamnava River basin primarily affects flood hazard [63],

while its impact on vulnerability within the study area is less pronounced, since most of the measures are implemented outside (i.e., upstream of) the ROI. Specifically, only a small portion of the area designated for afforestation falls within the ROI, as well as the floodplain restoration site and the Gračica retention pond. Nevertheless, owing to the fine spatial resolution of the calculation, M-FLOVI effectively captured the localized effects of these NbS measures.

5.2. Advantages, Limitations and Outlook

This study presents the application of M-FLOVI to assess vulnerability to floods in the Tamnava River basin, but M-FLOVI can be readily applied to other regions. Nevertheless, such applications would inevitably require some case-specific adjustments. The vulnerability assessments in this study were conducted in the region of interest (ROI), but M-FLOVI can be calculated at national or regional levels [87], or at the county, municipality or district level, which is particularly appealing for NbS applications in urban areas [88]. The resolution of the calculations has to be adjusted according to the task at hand. In this study, a rather fine resolution was adopted to ensure consistency with flood hazard, which was assessed as part of the RECONECT project, but coarser resolution (e.g., 1 km × 1 km) can be adopted, even in urban settings [88]. Adjustments are also needed regarding the data used for the indicator quantification. M-FLOVI is flexible and enables calculations with other data, including open-access data repositories, such as those listed in Table 2. M-FLOVI also allows calculations with datasets with higher spatial resolution (e.g., land cover data of 10 m × 10 m resolution instead of 100 m × 100 m [89]), or higher temporal resolution (for example, population data from continuously updated registers instead of decennial census data, as is the case in Norway [90]), where available.

The set of indicators can also be adjusted to accommodate locally relevant vulnerability drivers. For example, per capita income can be included in the income category of the economic vulnerability dimension, inhabitants aged between 0 and 4 years could be included in the demographic category [38], while both land use and land cover indicators can be used to quantify the natural category of the environmental vulnerability dimension. Data on socially vulnerable groups, such as locations of informal Roma settlements located in flood prone areas of the Tamnava River basin [91], can improve the accuracy of the social dimension estimates. Beyond adjustments to individual indicators, the five-dimension structure of M-FLOVI can itself be expanded. For instance, cultural heritage is currently subsumed within the social dimension but could be treated as a separate vulnerability dimension in contexts where its protection is of primary concern, such as heritage cities [88].

Special emphasis has to be placed on data translation to indicator values, which encompasses quantification (including the assignment of nominal values if needed) and normalization. This process is inherently case-specific: for example, the nominal values assigned to building types have to be compatible with the building typology of the study area, and those used in this study should be regarded only as indicative guidance. The weighting scheme may also be adjusted to reflect the preferences of local stakeholders and their vulnerability perceptions. Lastly, the thresholds used to classify the M-FLOVI values and create vulnerability maps may be adjusted (e.g., by applying the natural breaks approach).

Although flexible and widely applicable, M-FLOVI is accompanied by uncertainties stemming from each step of the calculation process. Uncertainties related to the processing of input data are especially pronounced. As shown in Table 2, data used for M-FLOVI calculation are rather heterogeneous: they carry different information, and may (e.g., buildings, traffic infrastructure) or may not be spatially explicit (e.g., the percentage of population without permanent income). Spatially explicit data can be either vectors of every type, or rasters, while quantitative datasets may differ by orders of magnitude. Therefore, homogenization of such

diverse datasets inevitably implies simplifications and uncertainties. For instance, buildings and traffic infrastructure, which are the datasets of finest spatial resolution used in this study, are obtained from the Google Maps and OpenStreet Maps and inherently contain positional uncertainties included in these maps [79,80].

Some datasets (e.g., those related to the demographic category, such as population without permanent income) are generally not available at high resolution. For example, these datasets were available only at the settlement level in the Tamnava River basin. Nevertheless, these datasets had to be disaggregated or downscaled to the pixel level to maintain consistency with other indicators and to enable M-FLOVI calculations. However, it should be noted that neither disaggregation nor downscaling refines the information content of the original data. In fact, both operations are inherently accompanied by considerable uncertainty. For example, residential building footprints represent a reasonable proxy for the downscaling of population count. However, the same proxy is poorly suited for downscaling population without permanent income, since this indicator exhibits higher underlying spatial variability than population count (even though both datasets are available only at the settlement level). Specifically, population without permanent income is often concentrated in socioeconomically disadvantaged areas (e.g., informal settlements), rather than evenly distributed across all residential buildings. Therefore, applying residential building-based downscaling can only introduce pseudo-resolution of this indicator and spuriously inflate vulnerability across pixels representing these buildings. For this reason, a simple disaggregation of this indicator to all pixels of the ROI was adopted in this study. Similar concerns apply to the demographic coefficient because building-based demographic data, such as residents' age or income, are not available in Serbia due to personal data protection legislation [92]. Extensive future research is needed to quantify uncertainty stemming from spatially redistributing these datasets, as well as to identify the optimal proxy dataset(s), especially bearing in mind that some form of spatial redistribution (whether disaggregation or downscaling) of demographic indicators is inevitable because of their nature. Specifically, these indicators, such as the self-help capacity, essentially represent a feature of a community (or a settlement) rather than an individual building or a pixel.

Bearing in mind that the ultimate objective of the vulnerability maps is identification of the most vulnerable areas within a study area and that vulnerability in every pixel of the study area is obtained with the same (uncertain) datasets, the impact of uncertainties on the relative comparison should be minimal. Nevertheless, it is essential that all datasets undergo thorough quality checks prior to vulnerability and flood risk assessments, since these uncertainties can further propagate and amplify throughout the calculation process [93].

Another source of uncertainty in input data processing is assigning nominal values based on the qualitative attributes of the dataset (e.g., building type). Although this process is case-specific, the nominal values, which basically represent a ranking, may be discriminatory due to rather large differences across the dataset [94]. However, these differences are expected to be mitigated through normalization. Normalization with respect to minimum and maximum values was adopted in this study, but the lowest value of the normalized indicator of ε is set to distinguish pixels with the normalized indicator with the value of zero from no-data pixels. This distinction is critical, as illustrated by the physical dimension of vulnerability. Specifically, pixels representing no buildings or traffic infrastructure have to be treated as no-data pixels in the physical dimension rather than assigned a vulnerability value, since the latter would produce a misleading vulnerability pattern in the study area.

To make this distinction, a value equal to 1% of the class width was adopted in this study, since preliminary considerations showed that such a small value cannot significantly affect the distribution of pixels among the vulnerability classes or their spatial

distribution. This is also illustrated by calculating the natural category in Section 3.2 (Equations (6) and (7)), which clearly shows that the impact of ε is minor, i.e., it affects only the fifth decimal place of the category. Similarly, calculating the demographic category in a hypothetical borderline pixel with the minimum value of ε for the population count indicator, which has the highest weight of 0.8 (Table 1), and maximum normalized values of 1 for the remaining two indicators (the demographic coefficient and the self-help capacity; Table 1) affects only the sixth decimal place of the resulting category value, which is comparable to the rounding errors in the quantification of indicators. Moreover, these impacts are expected to diminish further, as they get multiplied by weights smaller than one. Therefore, setting the minimum value ε merely enables capturing the vulnerability of a pixel, rather than omitting it as a no-data pixel, which is important in vulnerability assessments. However, other approaches to setting the thresholds among the categories can be tested (e.g., Z-normalization, normalization based on rankings or even fuzzy thresholds), as well as other approaches to handling no-data pixels. Even though previous research on this topic demonstrated a marginal contribution of normalization to the resulting vulnerability to floods [18], further research is needed to examine whether this finding holds for M-FLOVI and to assess the combined impacts of the nominal values and the normalization approach.

Setting the weights was one of the key challenges encountered during M-FLOVI development. As elaborated in Section 2, the weights used to calculate M-FLOVI were set from direct expert and stakeholder elicitation. Nevertheless, future research efforts can focus on gathering input from a larger number of stakeholders and experts, thereby enabling the assessment of weights through robust methods of multi-criteria decision analysis [95], such as MACBETH (Measuring Attractiveness by a Categorical Based Evaluation TecHnique), ELECTRE (ELimination and Choice Expressing REality) [96,97] or PROMETHEE (Preference Ranking Organization METHod for Enrichment Evaluations) [98–100]. Setting weights is essential for index-based vulnerability assessment, since different sets of weights can even lead to different decisions by stakeholders [23]. On the other hand, there are studies demonstrating that final vulnerability classes are primarily determined by the input data [47]. Therefore, extensive further research is needed to conduct sensitivity analyses and examine the impact of the M-FLOVI weights on its values and spatial distribution, with special emphasis on identification of the most vulnerable areas.

In this study, equal intervals were adopted to delineate between the four vulnerability classes (low, moderate, high and very high). This approach was adopted since previous research showed that it yields results comparable to those obtained by the natural breaks approach, which was singled out as the preferable approach to determining classification thresholds [18]. Nevertheless, the same study demonstrated a significant impact of the approach to setting the thresholds on the resulting vulnerability classes and their spatial distribution. Future research efforts are needed to examine if these findings also apply to M-FLOVI, especially bearing in mind that it builds on the weighted root sum of squares.

Uncertainties affecting vulnerability assessments under baseline conditions can further amplify under future scenarios, since they are additionally affected by inherent uncertainties in the future projections of land cover, population and commercial activities that shape different vulnerability categories and dimensions. Therefore, the plausibility of these projections has to be carefully examined before using them for assessments of future vulnerability to floods. Another challenge is the translation of these projections into the values of the affected indicators. For example, economic, social and institutional dimensions of vulnerability were kept constant across all scenarios in this study, since their adjustment is deemed more uncertain than keeping the baseline values. Such decisions are inherently case-specific and should be guided by the plausibility of the future projections and the

reliability of the underlying data, and all assumptions made in this process should be transparently documented.

The same challenge is valid when it comes to NbS implementation. Some NbSs and their effects simply cannot be captured by M-FLOVI. For instance, reforestation, obstacle removal or check dams for erosion control cannot be captured by M-FLOVI, as they do not affect any of its indicators. In its present form, M-FLOVI cannot capture NbS impacts on enhancing social cohesion or improvement of habitat quality (habitat connectivity) and biodiversity, which may reduce social and environmental vulnerability dimensions, respectively. Capturing these wider, profound NbSs' impacts on vulnerability to floods represents a genuine research gap that necessitates extensive future research. As indicated in Section 3.2, the economic implications of NbS implementation are rather challenging to assess (e.g., tourism, (green) job creation, increase in property values, energy savings, etc.) [101]. The M-FLOVI application in this study clearly revealed a localized increase in the environmental dimension of vulnerability due to floodplain restoration, which is expected to create a protected bird habitat. This particular NbS can even bring disbenefits in some instances, such as disruption of local livelihoods [101]. To ensure plausible future vulnerability assessments, it is essential to account for NbS disbenefits, as well as the dynamics of the NbSs' effects over time [102]. Another challenge to future vulnerability assessment is climate change, which can affect buildings [62,103], income [104], land cover [105,106], protected areas [107] and population [108,109] and, thus, influence vulnerability to floods.

6. Conclusions

This paper presents a novel Multi-dimensional Flood Vulnerability Index (M-FLOVI) built upon five vulnerability dimensions, each derived from carefully selected indicators sensitive to the impacts of nature-based solutions (NbSs) on future vulnerability. By systematically incorporating NbSs' impacts, M-FLOVI advances post-intervention flood risk assessments, of which vulnerability assessment is an integral part. The weighting scheme used to calculate M-FLOVI features great flexibility and can be easily adapted to enable applications across diverse regions with locally accessible data and to fit local conditions and stakeholders' preferences. It is readily implemented in a GIS environment, which facilitates M-FLOVI calculations, classifications and mapping, as well as combinations with flood hazard to assess and map flood risk.

The proposed method was applied to assess vulnerability to floods under the baseline and two future scenarios, without and with NbS measures planned for flood mitigation in the Tamnava River basin in Serbia. The most vulnerable areas identified under the baseline conditions correspond to those indicated in other vulnerability assessments and were the areas that indeed endured the most devastating consequences of the May 2014 flood. Our results show that the development of a photovoltaic power plant, as outlined in the municipalities' spatial plans, would increase vulnerability to floods. Conversely, the implementation of the proposed NbS measures (afforestation, retention ponds, floodplain restoration) would decrease vulnerability and, consequently, contribute to flood risk reduction. Interestingly, the proposed restoration of the abandoned Dokmir fishpond, which is expected to serve as a bird habitat with protection status upon its restoration, would locally increase the environmental dimension of vulnerability. These results demonstrate the soundness of M-FLOVI, which can detect both vulnerability reductions and increases in line with expected responses to the projected interventions. Moreover, NbSs were shown to contribute to flood risk reduction not only through flood hazard mitigation but also through vulnerability reduction. We, therefore, argue that future flood risk assessments should account for vulnerability changes and propose including NbSs' impacts on future vulnerability to floods in evaluations of their multifaceted effectiveness.

Author Contributions: Conceptualization, J.K.-M.; methodology, J.K.-M., A.T., N.R., and D.Š.; software, J.K.-M. and D.Š.; validation, J.K.-M., A.T., N.R., and D.Š.; formal analysis, J.K.-M. and D.Š.; investigation, J.K.-M., A.T., N.R. and D.Š.; resources, J.K.-M., A.T., N.R., D.Š. and V.Š.; data curation, J.K.-M. and D.Š.; writing—original draft preparation, J.K.-M.; writing—review and editing, J.K.-M., A.T., N.R., D.Š. and V.Š.; visualization, J.K.-M.; supervision, J.K.-M., A.T. and N.R.; project administration, N.R. All authors have read and agreed to the published version of the manuscript.

Funding: This research was funded from the European Union's Horizon 2020 research and innovation program under grant agreement No 776866 for the RECONECT (Regenerating ECOsystems with Nature-based solutions for hydro-meteorological risk rEduCTion) project. The study reflects only the authors' view, and the European Union is not liable for any use that may be made of the information contained herein. The Article Processing Charge (APC) was jointly funded by the Geographical Institute "Jovan Cvijić" of the Serbian Academy of Sciences and Arts and the Faculty of Civil Engineering, University of Belgrade, with each institution contributing 50% of the total expense.

Data Availability Statement: The open-access data used in this study are listed in Table 2 of the paper. The remaining data can be obtained from the authors upon request.

Acknowledgments: The research work of Jelena Kovačević-Majkić was supported by the Ministry of science, technological development and innovations of the Republic of Serbia (contract number 451-03-33/2026-03/200172). The authors gratefully acknowledge the guidance and support of Jasna Plavšić.

Conflicts of Interest: Author Mr. Vujica Šarenac was employed by IWA consulting from Belgrade, Serbia. The remaining authors declare that the research was conducted in the absence of any commercial or financial relationships that could be construed as a potential conflict of interest.

Abbreviations

The following abbreviations are used in this manuscript:

NbS	Nature-based solution
FRM	Flood risk management
ROI	Region of interest
ISPDR	The International Commission for the Protection of the Danube River
IMP	Immovable cultural properties
IPA	Instrument for Pre-accession Assistance
LC	Land cover
PA	Protected area
GIS	Geographical information system
QGIS	Quantum GIS
WRSS	Weighted Root Sum of Squares
UTM	Universal Transverse Mercator

Appendix A. The Index-Based Method Used to Calculate M-FLOVI

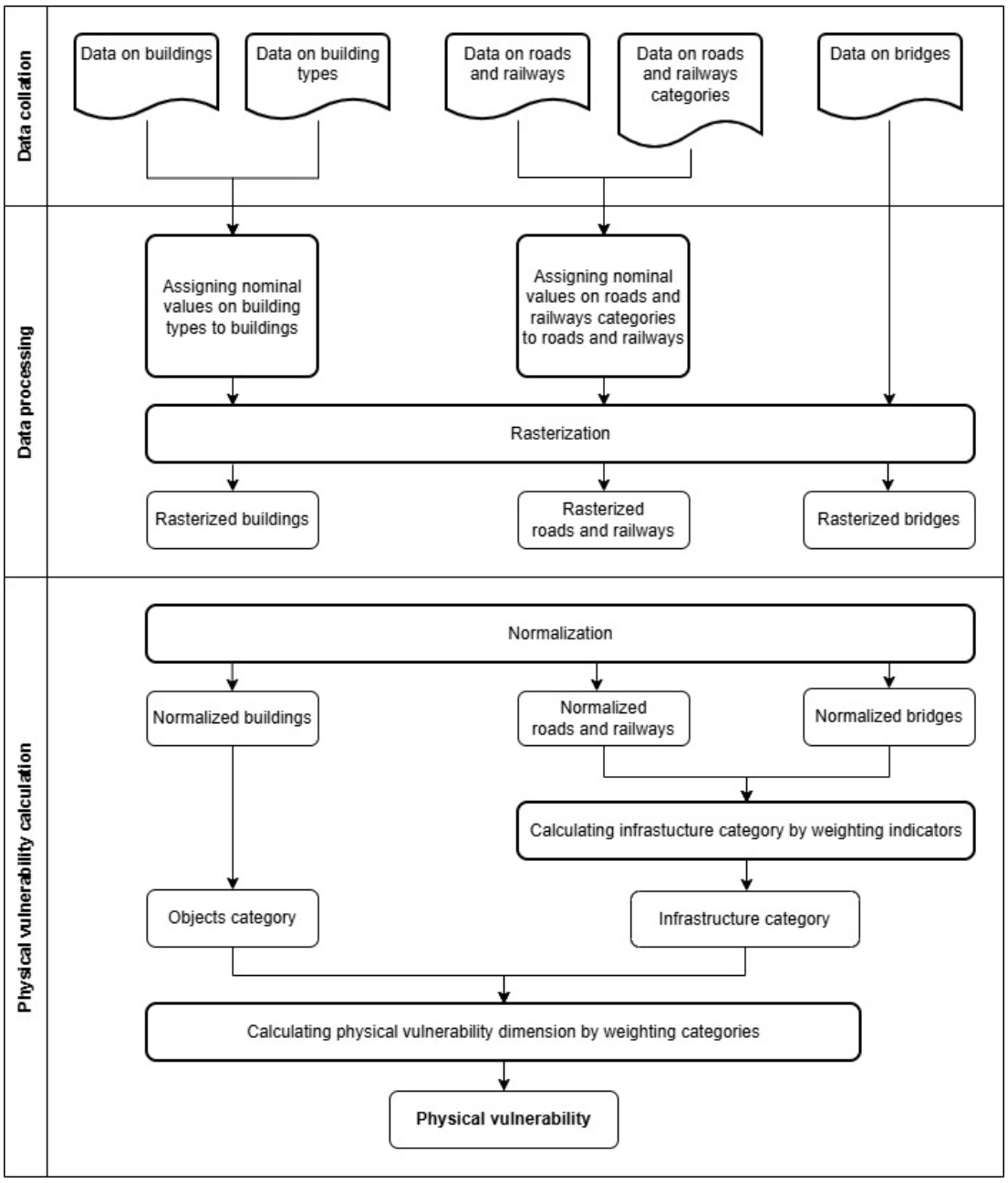

Figure A1. The M-FLOVI flowchart: the physical vulnerability dimension.

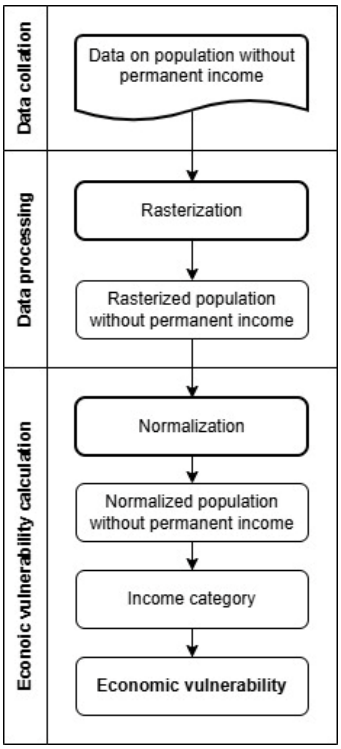

Figure A2. The M-FLOVI flowchart: the economic vulnerability dimension.

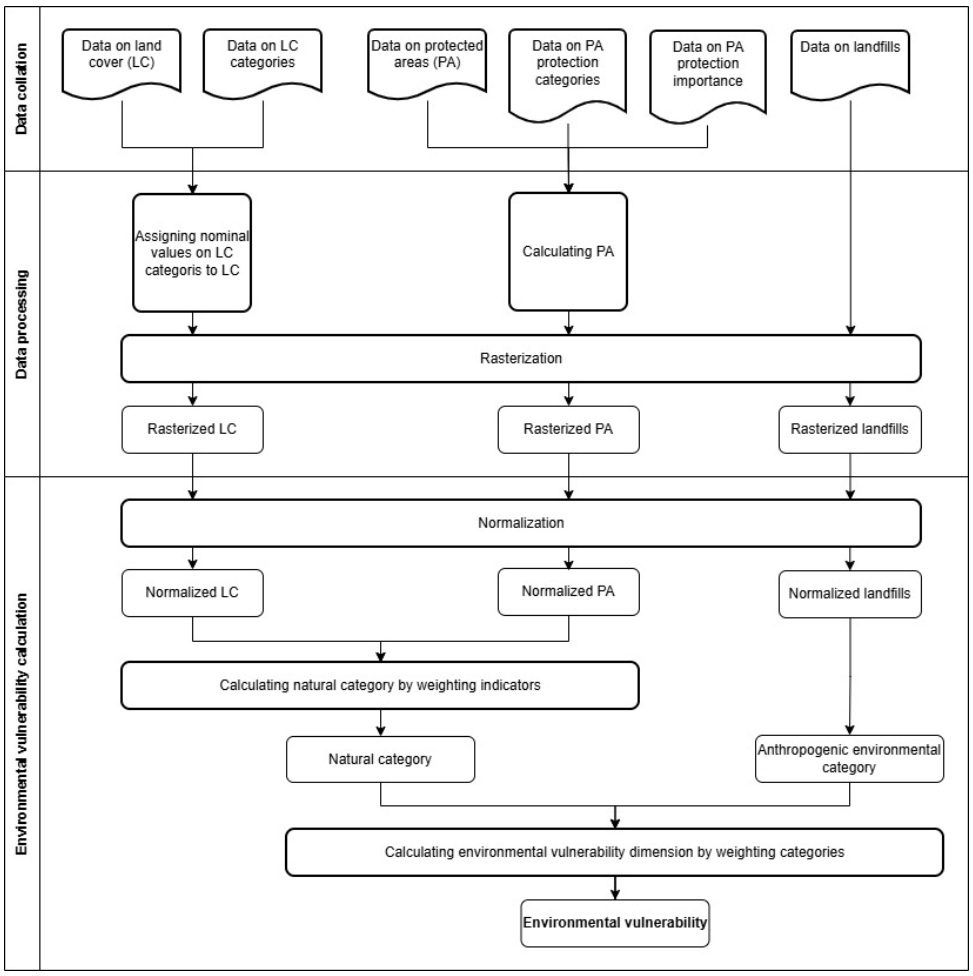

Figure A3. The M-FLOVI flowchart: the environmental vulnerability dimension.

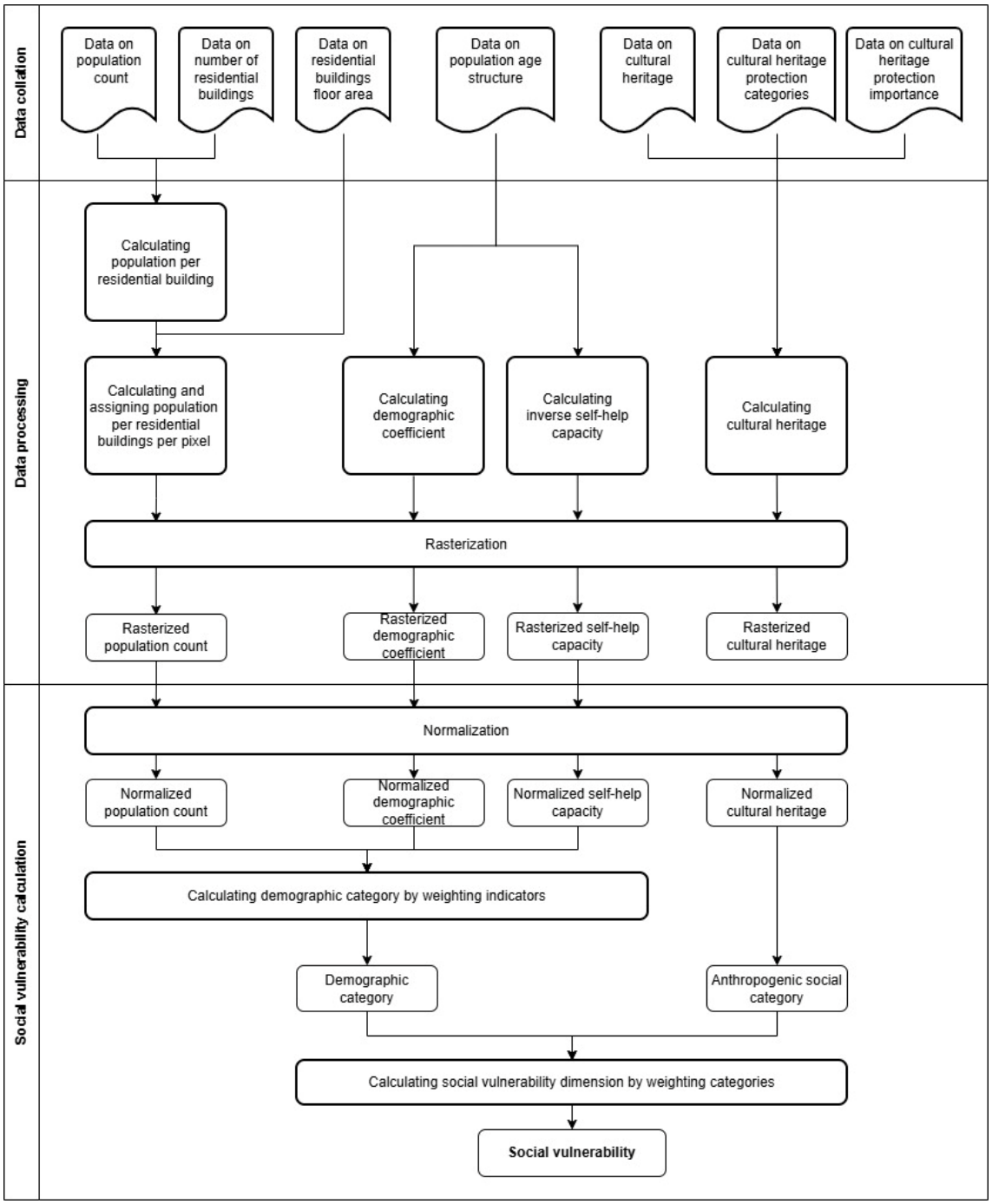

Figure A4. The M-FLOVI flowchart: the social vulnerability dimension.

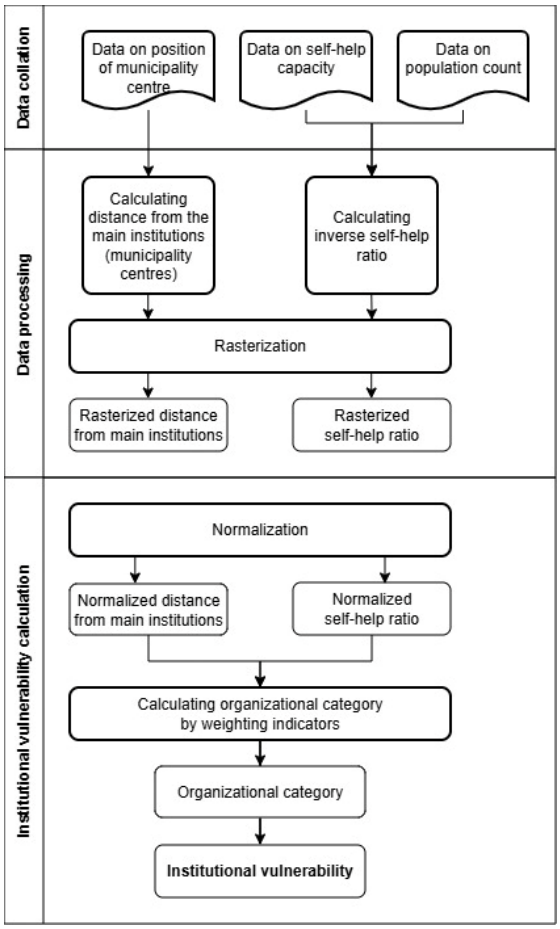

Figure A5. The M-FLOVI flowchart: the institutional vulnerability dimension.

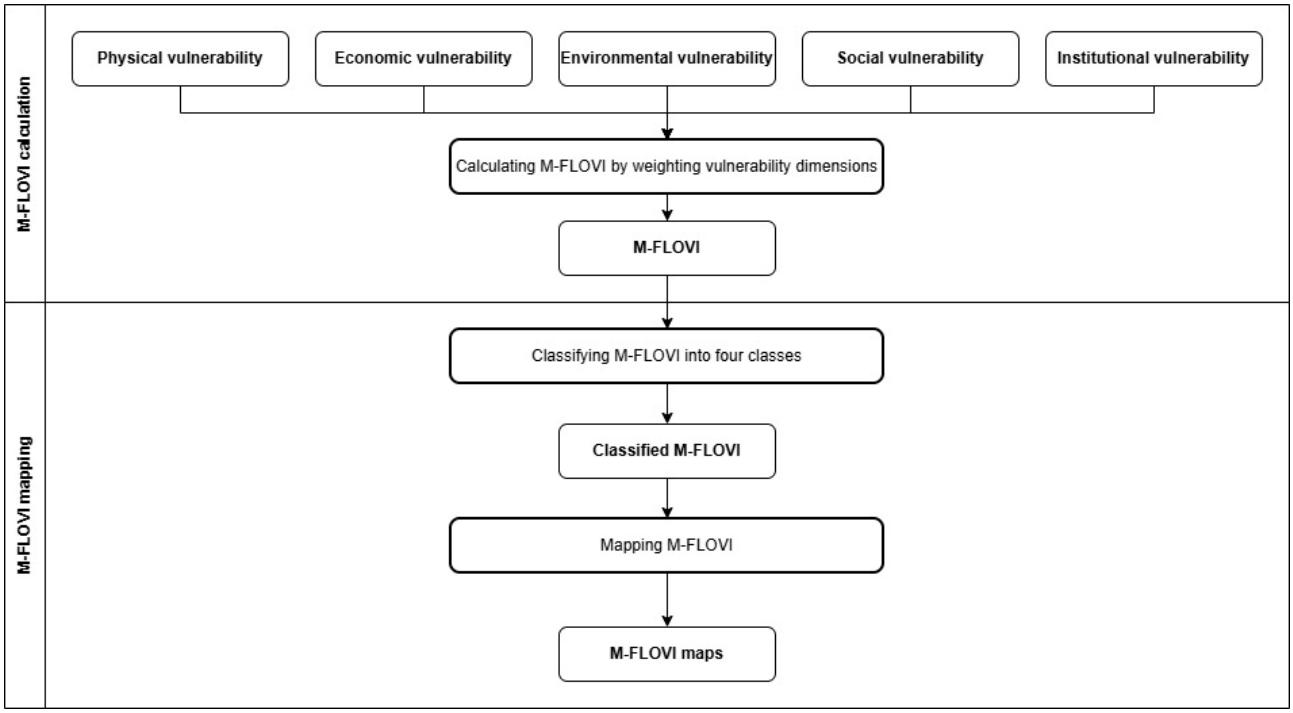

Figure A6. The M-FLOVI flowchart.

Appendix B. Indicators with Assigned Nominal Values for Vulnerability Assessment in the Tamnava River Basin

Table A1. Building types in the ROI in the Tamnava River basin and the corresponding nominal values.

Building Type	Nominal Values
Agricultural buildings—machines and livestock	2
Agricultural buildings—crops storage	1
Auxiliary buildings—garages, carports, undefined storage-type facilities	1
Commercial use	5
Educational use	5
Governmental use	5
Light industrial use	4
Institutional use	4
Energy facility	4
Residential: multi-family use	2
Residential: single family use, old-style traditional house, usually the oldest building on a multi-structure rural plot.	2
Residential: single family use, single-story (ground floor only)	3
Residential: single family use, up to two stories	2
Residential: single family use, up to three stories	2
Transportation hub buildings	1

Table A2. Transportation infrastructure and the corresponding nominal values.

Transportation Infrastructure	Category	Nominal Values
Roads	IA	5
	IB	4
	IIA	3
	IIB	2
Railways	N/A	5

Table A3. Land cover categories in the ROI in the Tamnava River basin and the corresponding nominal values.

Land Cover Category	Nominal Values
Water bodies	1
Wetlands	1
Forest and semi natural areas	2
Pastures	3
Agricultural areas	4
Artificial areas	5

Table A4. Protected areas (PA) categories in the ROI in the Tamnava River basin and the corresponding nominal values.

PA Category	Nominal Values
National Park	5
Nature Park	4
Outstanding natural landscape	3
Nature reserve	2
Natural monument	1
Protected habitat	1

Table A5. Cultural heritage represented by immovable cultural property (IMP) categories in the ROI in the Tamnava River basin and the corresponding nominal values.

IMP Category	Nominal Values
Cultural landscape	5
Special cultural-historical unit	4
Archaeological site	3
Landmark	2
Monument of culture	1

Table A6. Nominal values assigned to protected areas and cultural heritage according to their importance.

PA Importance	IMP Importance	Nominal Values According to the Importance Level
1st degree protection regime	IMP of exceptional importance	3
2nd degree protection regime	IMP of great importance	2
3rd degree protection regime	IMP	1

Appendix C. Vulnerability to Floods in the Tamnava River Basin

Table A7. Summary statistics of the M-FLOVI in the region of interest (ROI) within the Tamnava River basin under the baseline and future scenarios.

Statistics	Scenario		
	Baseline	S0 (Without NbSs)	S1 (With NbSs)
Mean	0.324	0.324	0.309
Maximum	0.777	0.777	0.762
Minimum	0.000	0.027	0.027
Range	0.777	0.750	0.735
Standard deviation	0.102	0.102	0.099
Coefficient of variation	0.316	0.316	0.321

Table A8. Vulnerability classes of M-FLOVI and its dimensions in the region of interest (ROI) under the baseline and future scenarios. The values in the table represent percentages of the ROI area, whereas the values in parentheses show percentage point change relative to the baseline conditions. Positive values indicate an increase relative to baseline.

Vulnerability Dimension	Vulnerability Class	Scenario		
		Baseline	S0 (Without NbSs)	S1 (With NbSs)
M-FLOVI	Low	15.76	15.77 (0.01)	19.94 (4.17)
	Moderate	83.48	83.42 (−0.06)	79.27 (−4.22)
	High	0.75	0.81 (0.06)	0.80 (0.05)
	Very high	2.5×10^3	2.5×10^3 (0)	2.5×10^3 (0)
Physical	No-data	99.49	99.43 (−0.06)	99.43 (−0.06)
	Low	0.29	0.29 (0)	0.29 (0)
	Moderate	0.18	0.18 (0)	0.18 (0)
	High	0.02	0.08 (0.06)	0.08 (0.06)
	Very high	0.02	0.02 (0)	0.02 (0)
Economic	Low	64.93	64.93	64.93
	Moderate	33.18	33.18	33.18
	High	1.17	1.17	1.17
	Very high	0.71	0.71	0.71
Environmental	Low	27.87	27.88 (0.01)	28.48 (0.61)
	Moderate	0.42	0.40 (−0.01)	0.70 (0.29)
	High	70.28	70.23 (−0.05)	69.33 (−0.95)
	Very high	1.44	1.49 (0.06)	1.49 (0.05)

Table A8. *Cont.*

Vulnerability Dimension	Vulnerability Class	Scenario		
		Baseline	S0 (Without NbSs)	S1 (With NbSs)
Social	Low	34.89	34.89	34.89
	Moderate	59.78	59.78	59.78
	High	5.33	5.33	5.33
	Very high	4.3×10^6	4.3×10^6	4.3×10^6
Institutional	Low	16.95	16.95	16.95
	Moderate	51.18	51.18	51.18
	High	30.28	30.28	30.28
	Very high	1.59	1.59	1.59

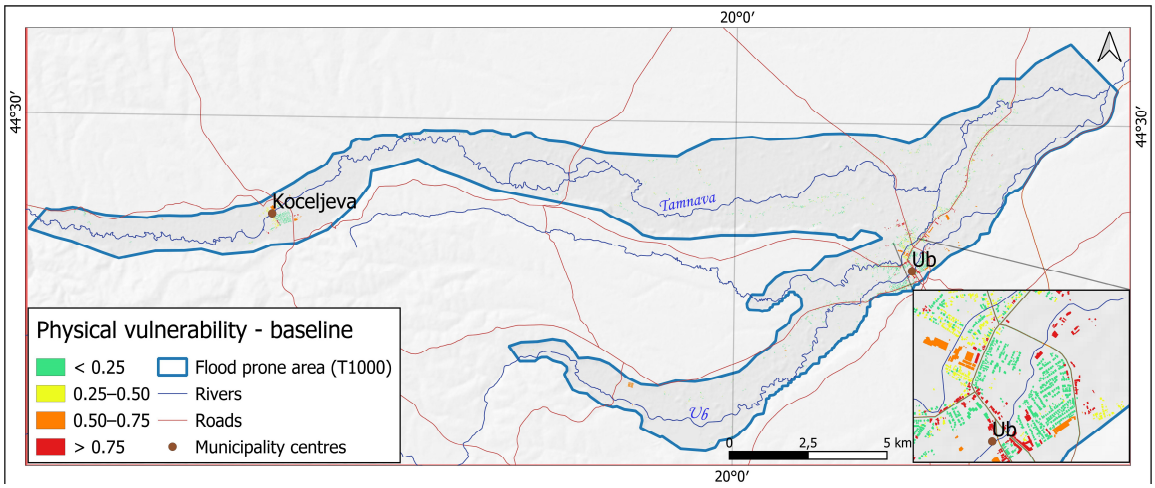

Figure A7. Physical vulnerability in the Tamnava River basin under the baseline conditions. Physical vulnerability in the vicinity of the town of Ub is shown in an enlarged inset in the bottom-right part of the figure. Gray areas indicate no-data, i.e., pixels containing no buildings or traffic infrastructure.

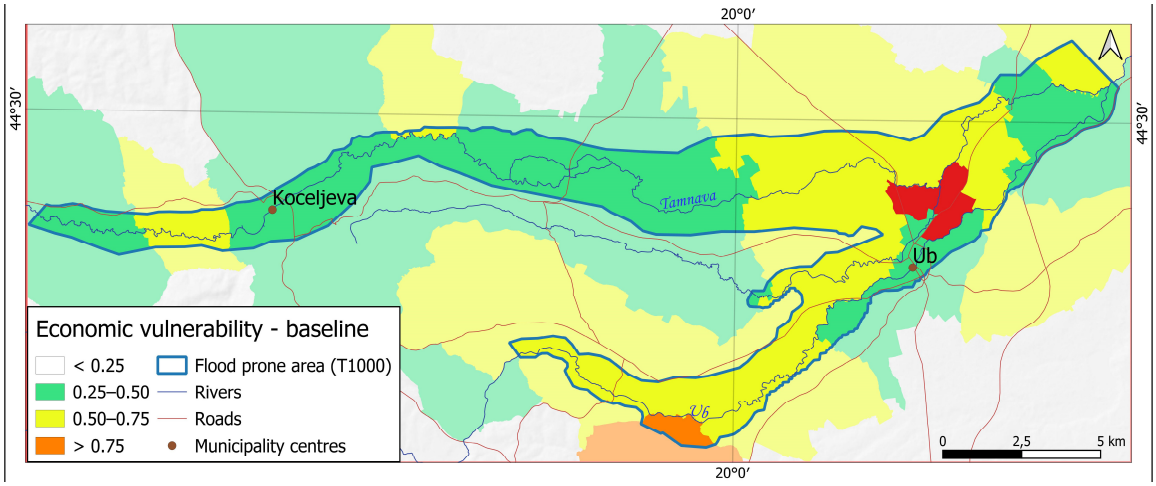

Figure A8. Economic vulnerability in the Tamnava River basin under the baseline conditions. The flood prone area is shown by more intense color tones than the remainder of the region of interest (ROI).

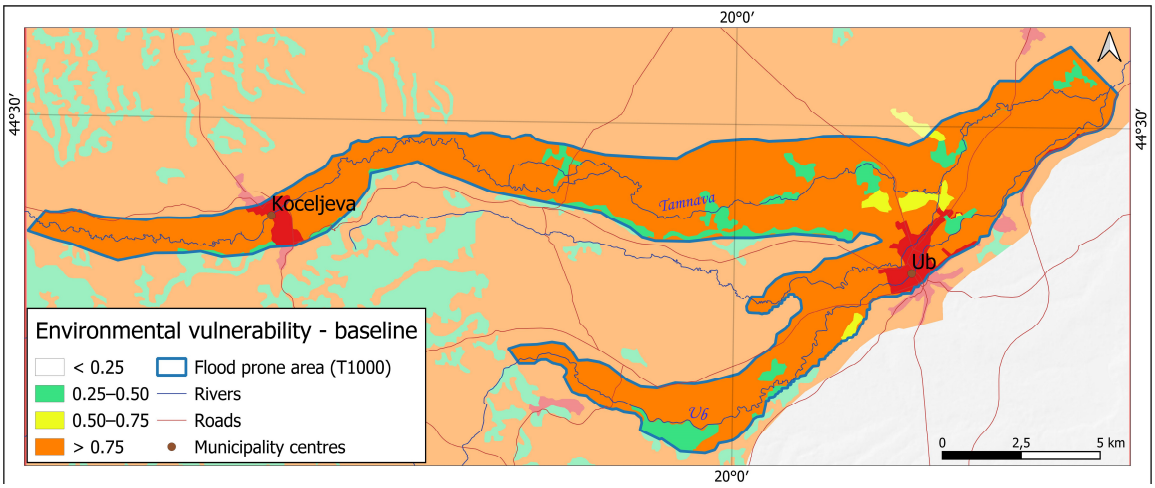

Figure A9. Environmental vulnerability in the Tamnava River basin under the baseline conditions. The flood prone area is shown by more intense color tones than the remainder of the region of interest (ROI).

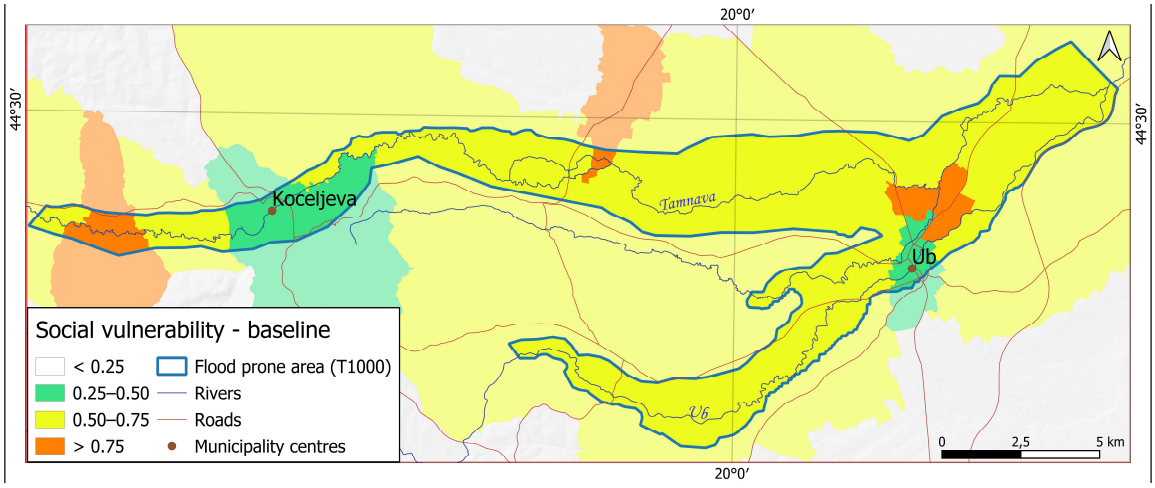

Figure A10. Social vulnerability in the Tamnava River basin under the baseline conditions. The flood prone area is shown by more intense color tones than the remainder of the region of interest (ROI).

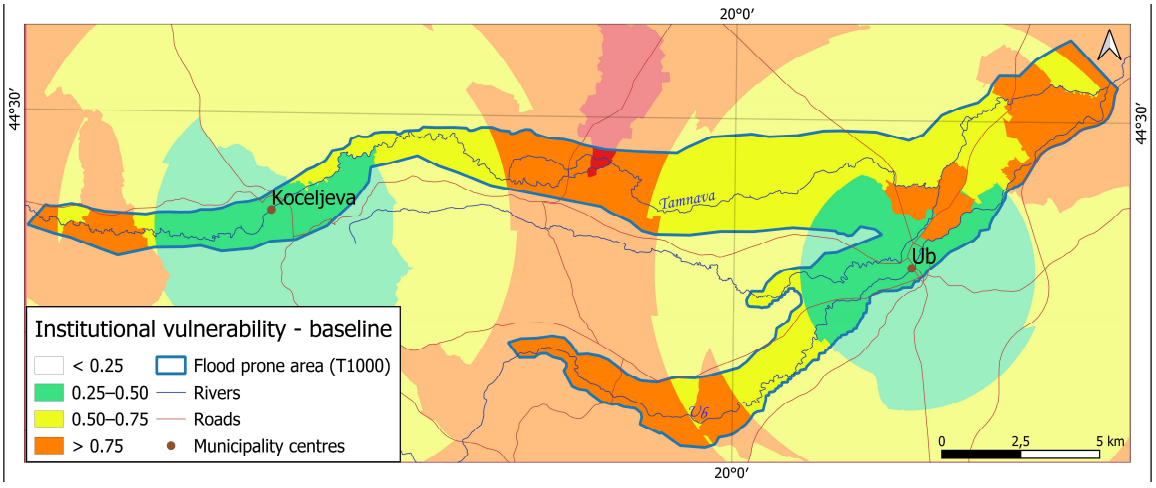

Figure A11. Institutional vulnerability in the Tamnava River basin under the baseline conditions. The flood prone area is shown by more intense color tones than the remainder of the region of interest (ROI).

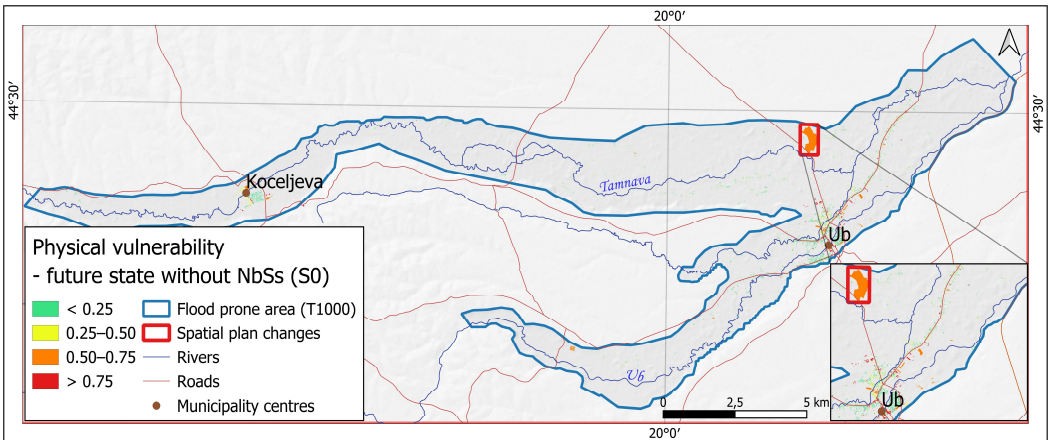

Figure A12. Physical vulnerability in the Tamnava River basin under the future S0 scenario ("without NbSs"). Red box indicates increased vulnerability due to projected land cover change.

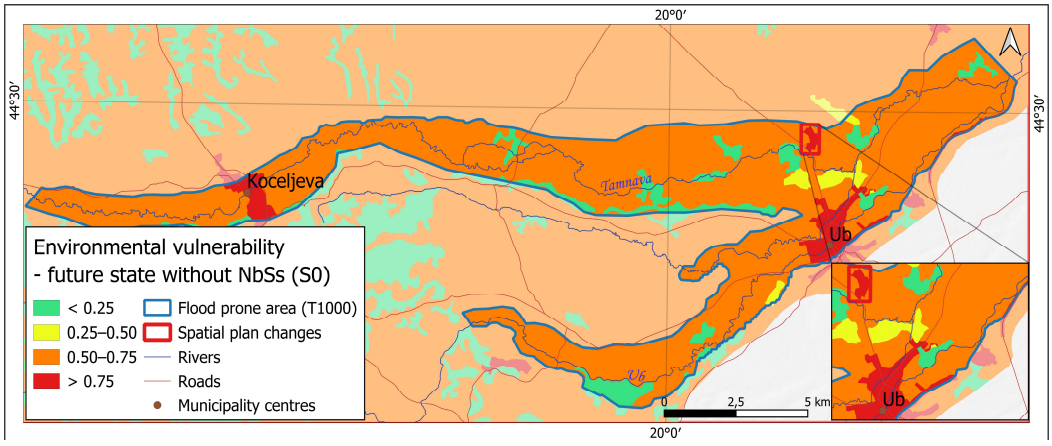

Figure A13. Environmental vulnerability in the Tamnava River basin under the future S0 scenario ("without NbSs"). Red box indicates increased vulnerability due to projected land cover change. The flood prone area is shown by more intense color tones than the remainder of the region of interest (ROI).

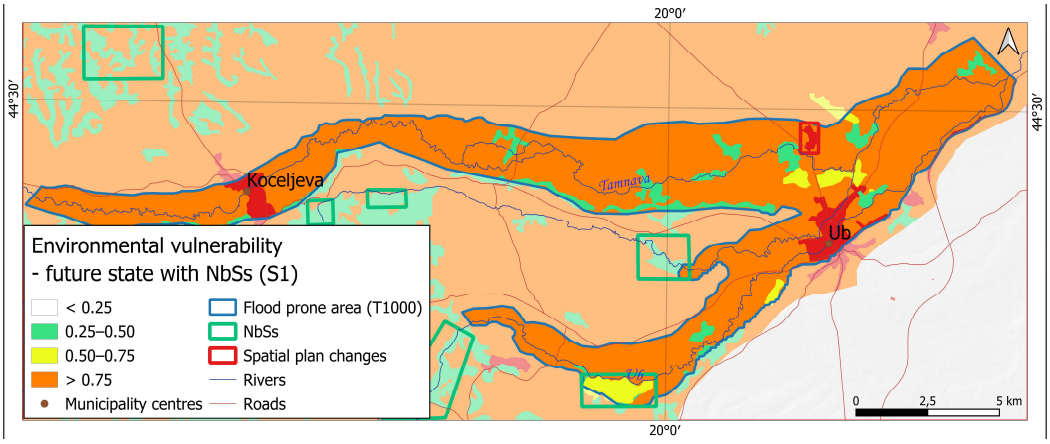

Figure A14. Environmental vulnerability in the Tamnava River basin under the future S1 scenario ("with NbSs"). Green boxes indicate areas of reduced vulnerability due to NbS implementation, while red box indicates increased vulnerability due to projected land cover change. The flood prone area is shown by more intense color tones than the remainder of the region of interest (ROI).

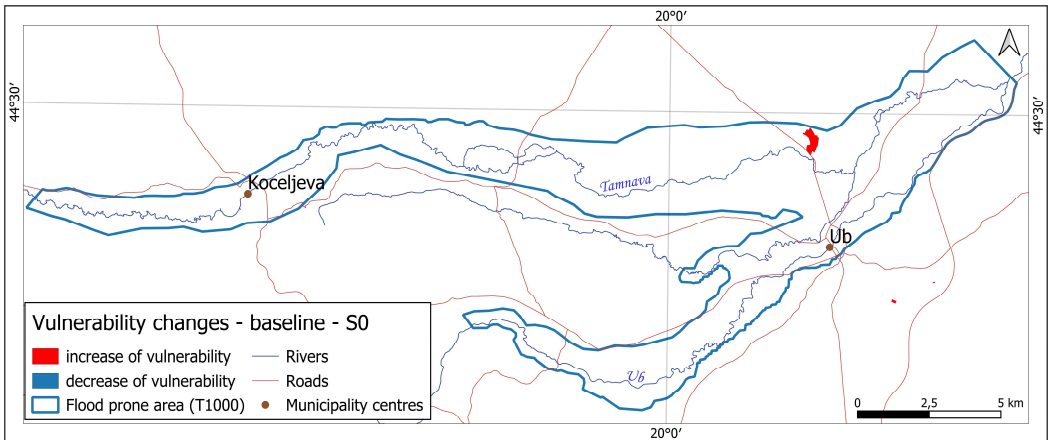

Figure A15. Change in vulnerability to floods under the future scenario S0 ("without NbSs") relative to the baseline conditions in the Tamnava River basin.

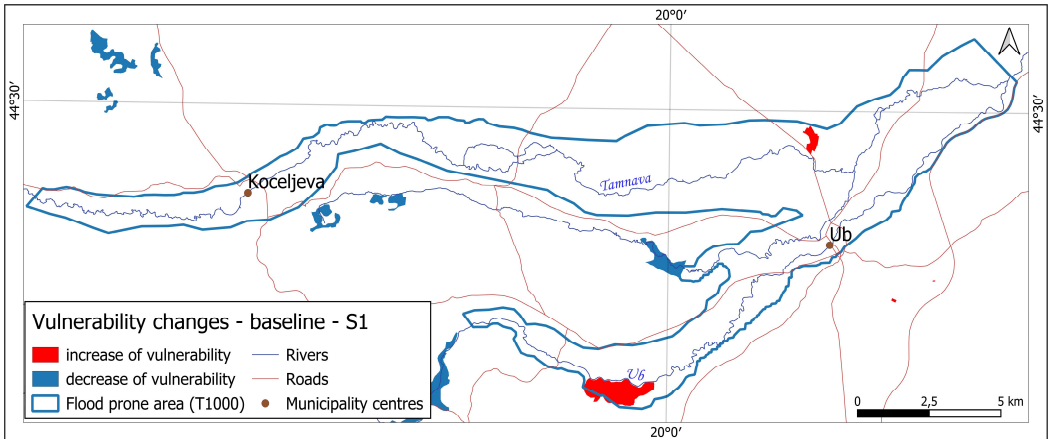

Figure A16. Change in vulnerability to floods under the future scenario S1 ("with NbSs") relative to the baseline conditions in the Tamnava River basin.

References

1. CRED-EM-DAT. 2025 Disasters in Numbers. Available online: https://files.emdat.be/reports/2025_EMDAT_report.pdf (accessed on 12 June 2026).
2. Delforge, D.; Wathelet, V.; Below, R.; Sofia, C.L.; Tonnelier, M.; Van Loenhout, J.A.F.; Speybroeck, N. EM-DAT: The Emergency Events Database. *Int. J. Disaster Risk Reduct.* **2025**, *124*, 105509. [CrossRef]
3. United Nations Office for Disaster Risk Reduction. *Global Assessment Report on Disaster Risk Reduction 2025: Resilience Pays: Financing and Investing for Our Future 2025*; UNDRR: Geneva, Switzerland, 2025; pp. 1–253.
4. EEA. Economic Losses from Weather- and Climate-Related Extremes in Europe. 2025. Available online: https://www.eea.europa.eu/en/analysis/indicators/economic-losses-from-climate-related (accessed on 15 October 2025).
5. Wisner, B.; Blaikie, P.; Cannon, T.; Davis, I. *At Risk: Natural Hazards, People's Vulnerability and Disasters*, 2nd ed.; Routledge: London, UK, 2004.
6. Kovačević-Majkić, J.; Miljanović, D.; Doljak, D. Spatial Aspects of Flood Exposure in Serbia. In *Water Resources Management: Methods, Applications and Challenges*; Nova Science Publishers, Inc.: New York, NY, USA, 2020; pp. 69–121.
7. Kron, W. Flood Risk = Hazard • Values • Vulnerability. *Water Int.* **2005**, *30*, 58–68. [CrossRef]
8. Boulange, J.; Hanasaki, N.; Yamazaki, D.; Pokhrel, Y. Role of Dams in Reducing Global Flood Exposure under Climate Change. *Nat. Commun.* **2021**, *12*, 417. [CrossRef] [PubMed]
9. Kim, K.; Han, D.; Kim, D.; Wang, W.; Jung, J.; Kim, J.; Kim, H.S. Combination of Structural Measures for Flood Prevention in Anyangcheon River Basin, South Korea. *Water* **2019**, *11*, 2268. [CrossRef]
10. El Karfa, D.; Al Karkouri, J.; Batchi, M.; Boudine, H. Assessing the Influence of the Al Wahda Dam Commissioning on Flood Flows and Low Water Levels in the Gharb Plain, Morocco. *J. Geogr. Inst. Jovan Cvijić SASA* **2024**, *74*, 273–280. [CrossRef]

11. Ruangpan, L.; Vojinovic, Z.; Di Sabatino, S.; Leo, L.S.; Capobianco, V.; Oen, A.M.P.; McClain, M.E.; Lopez-Gunn, E. Nature-Based Solutions for Hydro-Meteorological Risk Reduction: A State-of-the-Art Review of the Research Area. *Nat. Hazards Earth Syst. Sci.* **2020**, *20*, 243–270. [CrossRef]
12. Pudar, R.; Plavšić, J.; Todorović, A. Evaluation of Green and Grey Flood Mitigation Measures in Rural Watersheds. *Appl. Sci.* **2020**, *10*, 6913. [CrossRef]
13. Hansamali, U.; Makumbura, R.K.; Rathnayake, U.; Azamathulla, H.; Muttil, N. Leaky Dams as Nature-Based Solutions in Flood Management Part I: Introduction and Comparative Efficacy with Conventional Flood Control Infrastructure. *Hydrology* **2025**, *12*, 95. [CrossRef]
14. Shah, M.A.R.; Renaud, F.G.; Anderson, C.C.; Wild, A.; Domeneghetti, A.; Polderman, A.; Votsis, A.; Pulvirenti, B.; Basu, B.; Thomson, C.; et al. A Review of Hydro-Meteorological Hazard, Vulnerability, and Risk Assessment Frameworks and Indicators in the Context of Nature-Based Solutions. *Int. J. Disaster Risk Reduct.* **2020**, *50*, 101728. [CrossRef]
15. Shah, M.A.R.; Xu, J.; Carisi, F.; De Paola, F.; Di Sabatino, S.; Domeneghetti, A.; Gerundo, C.; Gonzalez-Ollauri, A.; Nadim, F.; Petruccelli, N.; et al. Quantifying the Effects of Nature-Based Solutions in Reducing Risks from Hydrometeorological Hazards: Examples from Europe. *Int. J. Disaster Risk Reduct.* **2023**, *93*, 103771. [CrossRef]
16. Birkmann, J.; Cardona, O.D.; Carreño, M.L.; Barbat, A.H.; Pelling, M.; Schneiderbauer, S.; Kienberger, S.; Keiler, M.; Alexander, D.; Zeil, P.; et al. Framing Vulnerability, Risk and Societal Responses: The MOVE Framework. *Nat. Hazards* **2013**, *67*, 193–211. [CrossRef]
17. Nasiri, H.; Mohd Yusof, M.J.; Mohammad Ali, T.A. An Overview to Flood Vulnerability Assessment Methods. *Sustain. Water Resour. Manag.* **2016**, *2*, 331–336. [CrossRef]
18. Moreira, L.L.; De Brito, M.M.; Kobiyama, M. Effects of Different Normalization, Aggregation, and Classification Methods on the Construction of Flood Vulnerability Indexes. *Water* **2021**, *13*, 98. [CrossRef]
19. Birkmann, J. Measuring Vulnerability to Promote Disaster-Resilient Societies: Conceptual Frameworks and Definitions. In *Measuring Vulnerability to Natural Hazards—Towards Disaster Resilient Societies*; UNU Press: Tokyo, Japan, 2006; pp. 9–54.
20. Kumpulainen, S. Vulnerability Concepts in Hazard and Risk Assessment. In *Natural and Technological Hazards and Risks Affecting the Spatial Development of European Regions*; Geological Survey of Finland: Espoo, Finland, 2006; pp. 65–74.
21. Zhang, Y.; Li, Z.; Xu, H.; Ge, W.; Qian, H.; Li, J.; Sun, H.; Zhang, H.; Jiao, Y. Impact of Floods on the Environment: A Review of Indicators, Influencing Factors, and Evaluation Methods. *Sci. Total Environ.* **2024**, *951*, 175683. [CrossRef] [PubMed]
22. Kaly, U.; Briguglio, L.; McLeod, H.; Schmall, S.; Pratt, C.; Pal, R. *Environmental Vulnerability Index (EVI) to Summarise National Environmental Vulnerability Profiles*; SOPAC: Suva, Fiji, 1999.
23. Papathoma-Köhle, M.; Schlögl, M.; Fuchs, S. Vulnerability Indicators for Natural Hazards: An Innovative Selection and Weighting Approach. *Sci. Rep.* **2019**, *9*, 15026. [CrossRef] [PubMed]
24. Aroca-Jiménez, E.; Bodoque, J.M.; García, J.A.; Figueroa-García, J.E. Holistic Characterization of Flash Flood Vulnerability: Construction and Validation of an Integrated Multidimensional Vulnerability Index. *J. Hydrol.* **2022**, *612*, 128083. [CrossRef]
25. Fernandez, P.; Mourato, S.; Moreira, M.; Pereira, L. A New Approach for Computing a Flood Vulnerability Index Using Cluster Analysis. *Phys. Chem. Earth Parts A/B/C* **2016**, *94*, 47–55. [CrossRef]
26. Cho, S.Y.; Chang, H. Recent Research Approaches to Urban Flood Vulnerability, 2006–2016. *Nat. Hazards* **2017**, *88*, 633–649. [CrossRef]
27. Moreira, L.L.; De Brito, M.M.; Kobiyama, M. Review Article: A Systematic Review and Future Prospects of Flood Vulnerability Indices. *Nat. Hazards Earth Syst. Sci.* **2021**, *21*, 1513–1530. [CrossRef]
28. Papathoma-Köhle, M.; Thaler, T.; Fuchs, S. An Institutional Approach to Vulnerability: Evidence from Natural Hazard Management in Europe. *Environ. Res. Lett.* **2021**, *16*, 044056. [CrossRef]
29. López-Martínez, F.; Gil-Guirado, S.; Pérez-Morales, A. Who Can You Trust? Implications of Institutional Vulnerability in Flood Exposure along the Spanish Mediterranean Coast. *Environ. Sci. Policy* **2017**, *76*, 29–39. [CrossRef]
30. Ginzarly, M.; Joshi, M.Y.; Teller, J. A Multidimensional Framework for Assessing Cultural Heritage Vulnerability to Flood Hazards. *Int. J. Herit. Stud.* **2024**, *30*, 1173–1192. [CrossRef]
31. Gandini, A.; Egusquiza, A.; Garmendia, L.; San-José, J.-T. Vulnerability Assessment of Cultural Heritage Sites towards Flooding Events. *IOP Conf. Ser. Mater. Sci. Eng.* **2018**, *364*, 012028. [CrossRef]
32. Beccari, B. A Comparative Analysis of Disaster Risk, Vulnerability and Resilience Composite Indicators. *PLoS Curr.* **2016**, *8*. [CrossRef] [PubMed]
33. Stenfors, E.; Blicharska, M.; Grabs, T.; Teutschbein, C. Multi-Sectoral and Systemic Drought Risk in Forested Cold Climates: Stakeholder-Informed Vulnerability Factors from Sweden. *Hydrol. Earth Syst. Sci.* **2025**, *29*, 3809–3832. [CrossRef]
34. Khan, A.; Gong, Z.; Shah, A.A.; Haq, M. A Multi-Criteria Decision-Making Approach to Vulnerability Assessment of Rural Flooding in Khyber Pakhtunkhwa Province, Pakistan. *Environ. Sci. Pollut. Res.* **2023**, *30*, 56786–56801. [CrossRef] [PubMed]
35. Khaldi, L.; Elabed, A.; Khanchoufi, A.E. Multidimensional Risk Assessment Based on Flood Susceptibility Mapping and Multiple Socioeconomic Variables under Climate Change. *Sci. Afr.* **2025**, *29*, e02834. [CrossRef]

36. Giurea, A.; Comănescu, L.; Dobre, R.; Nedelea, A.; Mirea, I. Flood Risk Assessment Using Multi-Criteria Spatial Analysis Case Study: Gilort River between Bălcești and Bolbocești. *Water* **2024**, *16*, 1760. [CrossRef]
37. Sulistyo, T.; Respati, S. The Estimation of Flood Area Based on a Few Selected and Weighted Parameters: Case Study of the Nangka River Basin, Balikpapan (Indonesia). *J. Geogr. Inst. Jovan Cvijić SASA* **2023**, *73*, 123–137. [CrossRef]
38. Moreira, L.L.; Vanelli, F.M.; Schwamback, D.; Kobiyama, M.; De Brito, M.M. Sensitivity Analysis of Indicator Weights for the Construction of Flood Vulnerability Indexes: A Participatory Approach. *Front. Water* **2023**, *5*, 970469. [CrossRef]
39. Ruangpan, L.; Vojinovic, Z.; Plavšić, J.; Curran, A.; Rosic, N.; Pudar, R.; Savic, D.; Brdjanovic, D. Economic Assessment of Nature-Based Solutions to Reduce Flood Risk and Enhance Co-Benefits. *J. Environ. Manag.* **2024**, *352*, 119985. [CrossRef] [PubMed]
40. Hufschmidt, G.A. A Comparative Analysis of Several Vulnerability Concepts. *Nat. Hazards* **2011**, *58*, 621–643. [CrossRef]
41. Kovačević-Majkić, J.; Panić, M.; Miljanović, D.; Miletić, R. Vulnerability to Natural Disasters in Serbia: Spatial and Temporal Comparison. *Nat. Hazards* **2014**, *72*, 945–968. [CrossRef]
42. Medina, N.; Abebe, Y.A.; Sanchez, A.; Vojinovic, Z. Assessing Socioeconomic Vulnerability after a Hurricane: A Combined Use of an Index-Based Approach and Principal Components Analysis. *Sustainability* **2020**, *12*, 1452. [CrossRef]
43. HANZE-Natural Hazards-Floods Database. Historical Floods with Impact Data (1870–2020). Available online: https://naturalhazards.eu/map (accessed on 24 February 2026).
44. Haubrock, P.J.; Stubbington, R.; Fohrer, N.; Hollert, H.; Jähnig, S.C.; Merz, B.; Pahl-Wostl, C.; Schüttrumpf, H.; Tetzlaff, D.; Wesche, K.; et al. A Holistic Catchment-Scale Framework to Guide Flood and Drought Mitigation Towards Improved Biodiversity Conservation and Human Wellbeing. *WIREs Water* **2025**, *12*, e70001. [CrossRef]
45. Štrbac, D. The Coefficient of Self-Help in a Relational Model Person-Natural Disaster. In *Proceedings of the Abstract Book*; University of Novi Sad, Faculty of Science, Department of Geography, Tourism and Hotel Management: Novi Sad, Serbia, 2012; pp. 27–28.
46. RECONECT. Available online: http://www.reconect.eu/network-of-cases/ (accessed on 5 November 2025).
47. Kovačević-Majkić, J. Procena Rizika od Bujičnih Poplava u Srbiji [Torrential Floods Assessment in Serbia]. Doctoral Dissertation, University of Belgrade, Belgrade, Serbia, 2018. (In Serbian)
48. Protection Civil. Directive 2007/60/EC on the European Parliament and of the Council on the Assessment and Management of Flood Risks (EU Flood Directive) 2007. *Off. J. Eur. Union* **2007**, *L288*, 27–34.
49. European Parliament; Council of the European Union. Directive 2007/2/EC of the European Parliament and of the Council Establishing an Infrastructure for Spatial Information in the European Community (INSPIRE) 2007. *Off. J. Eur. Union L* **2007**, *108*, 1–14.
50. O Metodologiji Izrade i Sadržaju Procene Rizika od Katastrofa i Plana Zaštite i Spasavanja [Instructions on the Methodology of the Creation and the Content of the Disaster Risk Assessment and Protection and Rescue Plan]. Available online: https://www.paragraf.rs/propisi/uputstvo-metodologiji-izradu-procene-ugrozenosti-elementarnih-nepogoda.html (accessed on 15 February 2026). (In Serbian)
51. Giupponi, C.; Mojtahed, V.; Gain, A.K.; Biscaro, C.; Balbi, S. Integrated Risk Assessment of Water-Related Disasters. In *Hydro-Meteorological Hazards, Risks and Disasters*; Elsevier: Amsterdam, The Netherlands, 2015; pp. 163–200. ISBN 978-0-12-394846-5.
52. Karagiorgos, K.; Thaler, T.; Heiser, M.; Hübl, J.; Fuchs, S. Integrated Flash Flood Vulnerability Assessment: Insights from East Attica, Greece. *J. Hydrol.* **2016**, *541*, 553–562. [CrossRef]
53. Lechowska, E. What Determines Flood Risk Perception? A Review of Factors of Flood Risk Perception and Relations between Its Basic Elements. *Nat. Hazards* **2018**, *94*, 1341–1366. [CrossRef]
54. Röthlisberger, V.; Zischg, A.P.; Keiler, M. Identifying Spatial Clusters of Flood Exposure to Support Decision Making in Risk Management. *Sci. Total Environ.* **2017**, *598*, 593–603. [CrossRef] [PubMed]
55. Devi, K.; Reddy, C.C.; Rahul, K.; Khuntia, J.R.; Das, B.S. A Holistic Methodology for Evaluating Flood Vulnerability, Generating Flood Risk Map and Conducting Detailed Flood Inundation Assessment. *Sci. Rep.* **2025**, *15*, 28253. [CrossRef] [PubMed]
56. Malgwi, M.B.; Schlögl, M.; Keiler, M. Expert-Based versus Data-Driven Flood Damage Models: A Comparative Evaluation for Data-Scarce Regions. *Int. J. Disaster Risk Reduct.* **2021**, *57*, 102148. [CrossRef]
57. Oulahen, G.; Mortsch, L.; Tang, K.; Harford, D. Unequal Vulnerability to Flood Hazards: "Ground Truthing" a Social Vulnerability Index of Five Municipalities in Metro Vancouver, Canada. *Ann. Assoc. Am. Geogr.* **2015**, *105*, 473–495. [CrossRef]
58. Ruangpan, L.; Vojinovic, Z.; Plavšić, J.; Doong, D.-J.; Bahlmann, T.; Alves, A.; Tseng, L.-H.; Randelović, A.; Todorović, A.; Kocic, Z.; et al. Incorporating Stakeholders' Preferences into a Multi-Criteria Framework for Planning Large-Scale Nature-Based Solutions. *Ambio* **2021**, *50*, 1514–1531. [CrossRef] [PubMed]
59. RECONECT. D4.2: Report Describing Baseline Assessment and Potential for NBS in Collaborators. Available online: http://www.reconect.eu/wp-content/uploads/2024/10/D4-2-Report-describing-baseline-assessment-and-potential-for-NBS-in-Collaborators.pdf (accessed on 12 May 2025).
60. European Commission; Joint Research Centre. *Global Flood Depth-Damage Functions: Methodology and the Database with Guidelines*; Publications Office: Luxembourg, 2016.

61. Scheuer, S.; Haase, D.; Meyer, V. Exploring Multicriteria Flood Vulnerability by Integrating Economic, Social and Ecological Dimensions of Flood Risk and Coping Capacity: From a Starting Point View towards an End Point View of Vulnerability. *Nat. Hazards* **2011**, *58*, 731–751. [CrossRef]
62. Ng, W.-S. Impact of Climate Change on Infrastructure. In *Industry, Innovation and Infrastructure*; Leal Filho, W., Azul, A.M., Brandli, L., Lange Salvia, A., Wall, T., Eds.; Encyclopedia of the UN Sustainable Development Goals; Springer International Publishing: Cham, Switzerland, 2021; pp. 489–497. ISBN 978-3-319-95872-9.
63. RECONECT. Available online: http://www.reconect.eu/public-deliverables/ (accessed on 5 November 2025).
64. Stanić, F.G.; Plavšić, J.; Todorović, A.; Rosić, N. Universal Flood Risk Reduction Index (FRRI) for Evaluating Effectiveness of Nature-Based Solutions. Book of Abstracts "Bridging Science and Practice" (C2-1). In Proceedings of the Nature-Based Solutions for Water Security and Climate Adaptation, Belgrade, Serbia, 3–5 July 2024; Available online: https://cris.vub.be/ws/portalfiles/portal/121690389/handbook_of_abstracts.pdf (accessed on 20 June 2026).
65. Vlada Republike Srbije [Government of the Republic of Serbia]. Poplave u Srbiji 2014 [Floods in Serbia in 2014]. 2014. Available online: https://www.obnova.gov.rs/uploads/useruploads/Documents/Izvestaj-o-proceni-potreba-za-oporavak-i-obnovu-posledica-poplava.pdfhttps://www.obnova.gov.rs/uploads/useruploads/Documents/Izvestaj-o-proceni-potreba-za-oporavak-i-obnovu-posledica-poplava.pdf (accessed on 30 June 2026). (In Serbian)
66. Stanić, M.; Todorović, A.; Vasilić, Ž.; Plavšić, J. Extreme Flood Reconstruction by Using the 3DNet Platform for Hydrological Modelling. *J. Hydroinformatics* **2018**, *20*, 766–783. [CrossRef]
67. Langović, M.; Srećković, V.; Vidović, Z.; Langović, M.; Mijić, Z. The Nexus between Solar Activity and Population Displacement: The Case Study of Southern Europe. *J. Geogr. Inst. Jovan Cvijić SASA* **2025**, *75*, 329–345. [CrossRef]
68. Filipović, I.; Gagić, N.; Rodin, V.; Avramović, V. *Interpretation of Geological Map 1:100000, Sheet Vladimirci 1973*; Federal Geologic Survey: Belgrade, Yugoslavia, 1973.
69. Pudar, R.; Ivetić, M.; Plavšić, J. Valuation of Fluvial Ecosystems in Function of Flood Protection: The Tamnava River Watershed Example. *Vodoprivreda* **2021**, *53*, 131–142.
70. HEC-RAS User's Manual. Available online: https://www.hec.usace.army.mil/confluence/rasdocs/rasum/latest (accessed on 10 June 2026).
71. Todorović, A.; Stanić, M.; Vasilić, Z.; Plavšić, J. The 3DNet-Catch Hydrologic Model: Development and Evaluation. *J. Hydrol.* **2019**, *568*, 26–45. [CrossRef]
72. Government of the Republic of Serbia. *Official Gazette RS 105/2013, 119/2013, 93/2015. Uredba o Kategorizaciji Državnih Puteva [Road Category Classification]*; Official Gazette: Belgrade, Serbia, 2015; Available online: https://www.paragraf.rs/propisi/uredba-kategorizaciji-drzavnih-puteva.html (accessed on 20 June 2026). (In Serbian)
73. Statistical Office of the Republic of Serbia. Census 2022—Population Database. Available online: https://popis2022.stat.gov.rs/en-us/https://popis2022.stat.gov.rs/en-us/ (accessed on 30 November 2023).
74. EEA. CORINE 2018. (Raster 100 m). 2020. Available online: https://sdi.eea.europa.eu/catalogue/copernicus/api/records/960998c1-1870-4e82-8051-6485205ebbac?language=all (accessed on 21 June 2026).
75. SEPA (Serbian Environmental Protection Agency). Landfills in Serbia. Available online: http://77.46.150.221/kdd/ (accessed on 20 June 2026).
76. GeoSrbija–National Infrastructure of Geospatial Data. Zaštićena Prirodna Dobra [Natural Protected Areas]. Available online: https://a3.geosrbija.rs/zasticena_podrucja (accessed on 15 December 2023).
77. QGIS Development Team. QGIS Geographic Information System (Version 3.34). 2024. Available online: http://www.qgis.orghttp://www.qgis.org (accessed on 10 June 2026).
78. Google LLC-Google Maps. Map of Serbia (Cloud Score+ Satellite and Expanded Street View). Available online: https://www.google.com/maps/@44.4896438,19.9234206,40662m/data=!3m1!1e3?authuser=0&entry=ttu&g_ep=EgoyMDI2MDYyMS4wIKXMDSoASAFQAw== (accessed on 25 June 2024).
79. El-Ashmawy, K.L.A. Testing the Positional Accuracy of OpenStreetMap Data for Mapping Applications. *Geod. Cartogr.* **2016**, *42*, 25–30. [CrossRef]
80. OpenStreetMap Contributors. Map of Serbia. Available online: https://www.openstreetmap.org (accessed on 25 June 2024).
81. Zavod za Zaštitu Prirode [Institute for Nature Protection of Serbia], Zaštićena Prirodna Dobra [Protected Areas]. Available online: https://zzps.rs/ (accessed on 19 June 2026). (In Serbian)
82. Institute for the Protection of Cultural Monuments. Informacioni Sistem Nepokretnih Kulturnih Dobara [Information System of Immovable Cultural Properties]. Available online: https://nasledje.gov.rs/index.cfm?jezik=Engleski (accessed on 14 June 2026).
83. Government of the Republic of Serbia. *Official Gazzette RS 36/2009, 88/2010, 91/2010-Corrected, 14/2016, 95/2018-and 71/2021. Zakon o Zaštiti Prirode [Law on Nature Protection]*; Official Gazette: Belgrade, Serbia, 2021; Available online: https://www.paragraf.rs/propisi/zakon_o_zastiti_prirode.html (accessed on 18 January 2024). (In Serbian)
84. Raković, M.; Novaković, B. Fauna Ptica Ribnjaka "Dokmir" [Avifauna of Dokmir Fishpond]. *J. Bird Prot. Study Soc. Vojv.* **2003**, *12*, 121–129.

85. Panić, M. *Social Vulnerability to Natural Hazards in Serbia*; Geographical Institute "Jovan Cvijić" SASA: Belgrade, Serbia, 2022. (In Serbian)
86. PWMC "Srbijavode". Karte Ugroženosti i Karte Rizika Od Poplava [Flood Hazard and Flood Risk Maps]. Available online: https://www.srbijavode.rs/karte-ugrozenosti-i-karte-rizika-od-poplava.html (accessed on 20 March 2026).
87. Ali, R.; Sajjad, H.; Rahaman, M.H.; Saha, T.K.; Masroor, M.; Roshani; Sharma, A. A Systematic Review on Climate Change-Induced Flood Susceptibility, Vulnerability and Risk: Future Research Perspective. *Environ. Monit. Assess.* **2025**, *197*, 1127. [CrossRef] [PubMed]
88. Li, J.; Zhang, Y.; Liu, K.; Zhao, J.; Wang, M. Integrating Nature-Based Solutions into Heritage-Sensitive Flood Risk Management: A Case Study of Liwan District, Guangzhou. *Urban Clim.* **2026**, *67*, 102919. [CrossRef]
89. Venter, Z.S.; Sydenham, M.A.K. Continental-Scale Land Cover Mapping at 10 m Resolution Over Europe (ELC10). *Remote Sens.* **2021**, *13*, 2301. [CrossRef]
90. Statistic Norway. *Population and Housing Census 2011. International-Different Methods-Comparable Results*; Statistics Norway: Oslo, Norway; Kongsvinger, Norway, 2011.
91. Vuksanović-Macura, Z. The Mapping and Enumeration of Informal Roma Settlements in Serbia. *Environ. Urban.* **2012**, *24*, 685–705. [CrossRef]
92. Government of the Republic of Serbia. *Official Gazette RS 87/2018. Zakon o Zaštiti Podataka o Ličnosti [Law on Personal Data Protection]*; Official Gazette: Belgrade, Serbia, 2018; Available online: https://www.paragraf.rs/propisi/zakon_o_zastiti_podataka_o_licnosti.htmlhttps://www.paragraf.rs/propisi/zakon_o_zastiti_podataka_o_licnosti.html (accessed on 20 June 2026). (In Serbian)
93. Saisana, M.; Saltelli, A.; Tarantola, S. Uncertainty and Sensitivity Analysis Techniques as Tools for the Quality Assessment of Composite Indicators. *J. R. Stat. Soc. Ser. A Stat. Soc.* **2005**, *168*, 307–323. [CrossRef]
94. Topalović, Ž.; Todorović, A.; Plavšić, J. Evaluating the Transferability of Monthly Water Balance Models under Changing Climate Conditions. *Hydrol. Sci. J.* **2020**, *65*, 928–950. [CrossRef]
95. de Brito, M.M.; Evers, M. Multi-Criteria Decision-Making for Flood Risk Management: A Survey of the Current State of the Art. *Nat. Hazards Earth Syst. Sci.* **2016**, *16*, 1019–1033. [CrossRef]
96. Bana, E.; Costa, C.A.; Antão Da Silva, P.; Nunes Correia, F. Multicriteria Evaluation of Flood Control Measures: The Case of Ribeira Do Livramento. *Water Resour. Manag.* **2004**, *18*, 263–283. [CrossRef]
97. Bosquet, M. MCDA for NBS: A Transdisciplinary Approach Combining Multicriteria Decision Analysis and Nature-Based Solution Planning. Doctoral Dissertation, Laval University, Quebec, QC, Canada, 2024.
98. Plataridis, K.; Mallios, Z. Mapping Flood Susceptibility with PROMETHEE Multi-Criteria Analysis Method. *Environ. Sci. Pollut. Res.* **2024**, *31*, 41267–41289. [CrossRef] [PubMed]
99. Dadrasajirlou, Y.; Karami, H.; Mirjalili, S. Using AHP-PROMOTHEE for Selection of Best Low-Impact Development Designs for Urban Flood Mitigation. *Water Resour. Manag.* **2023**, *37*, 375–402. [CrossRef]
100. Soldati, A.; Chiozzi, A.; Nikolić, Ž.; Vaccaro, C.; Benvenuti, E. A PROMETHEE Multiple-Criteria Approach to Combined Seismic and Flood Risk Assessment at the Regional Scale. *Appl. Sci.* **2022**, *12*, 1527. [CrossRef]
101. Ommer, J.; Bucchignani, E.; Leo, L.S.; Kalas, M.; Vranić, S.; Debele, S.; Kumar, P.; Cloke, H.L.; Di Sabatino, S. Quantifying Co-Benefits and Disbenefits of Nature-Based Solutions Targeting Disaster Risk Reduction. *Int. J. Disaster Risk Reduct.* **2022**, *75*, 102966. [CrossRef]
102. Asl, S.R.; Tate, E.; Pearsall, H. SECURE-NBS: A Conceptual Framework for Integrated Nature-Based Flood Risk Reduction. *Landsc. Urban Plan.* **2026**, *271*, 105637. [CrossRef]
103. Jiang, A.; Liu, X.; Czarnecki, E.; Zhang, C. Hourly Weather Data Projection Due to Climate Change for Impact Assessment on Building and Infrastructure. *Sustain. Cities Soc.* **2019**, *50*, 101688. [CrossRef]
104. Gilli, M.; Calcaterra, M.; Emmerling, J.; Granella, F. Climate Change Impacts on the Within-Country Income Distributions. *J. Environ. Econ. Manag.* **2024**, *127*, 103012. [CrossRef]
105. IPCC. Summary for Policymakers. In *Climate Change and Land: An IPCC Special Report on Climate Change, Desertification, Land Degradation, Sustainable Land Management, Food Security, and Greenhouse Gas Fluxes in Terrestrial Ecosystems*; IPCC: Geneva, Switzerland, 2022.
106. Barati, A.A.; Zhoolideh, M.; Azadi, H.; Lee, J.-H.; Scheffran, J. Interactions of Land-Use Cover and Climate Change at Global Level: How to Mitigate the Environmental Risks and Warming Effects. *Ecol. Indic.* **2023**, *146*, 109829. [CrossRef]
107. Hannah, L. Protected Areas and Climate Change. *Ann. N. Y. Acad. Sci.* **2008**, *1134*, 201–212. [CrossRef] [PubMed]

108. Stephenson, J.; Newman, K.; Mayhew, S. Population Dynamics and Climate Change: What Are the Links? *J. Public Health* **2010**, *32*, 150–156. [CrossRef] [PubMed]
109. Maja, M.M.; Ayano, S.F. The Impact of Population Growth on Natural Resources and Farmers' Capacity to Adapt to Climate Change in Low-Income Countries. *Earth Syst. Environ.* **2021**, *5*, 271–283. [CrossRef]

Disclaimer/Publisher's Note: The statements, opinions and data contained in all publications are solely those of the individual author(s) and contributor(s) and not of MDPI and/or the editor(s). MDPI and/or the editor(s) disclaim responsibility for any injury to people or property resulting from any ideas, methods, instructions or products referred to in the content.